AD_____

Award Number: W81XWH-04-1-0494

TITLE: GSK-3/Rb12 Pathway as a Novel Target of Rapamycin in Prostate Cancer

PRINCIPAL INVESTIGATOR: Larisa Litovchick, M.D., Ph.D.

CONTRACTING ORGANIZATION: Dana Farber Cancer Institute
Boston, MA 02115

REPORT DATE: November 2005

TYPE OF REPORT: Annual Summary

PREPARED FOR: U.S. Army Medical Research and Materiel Command
Fort Detrick, Maryland 21702-5012

REPORT DOCUMENTATION PAGE

Form Approved
OMB No. 0704-0188

1. REPORT DATE *(DD-MM-YYYY)*	**2. REPORT TYPE**	**3. DATES COVERED** *(From - To)*
01-11-2005	Annual Summary	15 Apr 2004 – 14 Oct 2005

4. TITLE AND SUBTITLE
GSK-3/Rb12 Pathway as a Novel Target of Rapamycin in Prostate Cancer

5a. CONTRACT NUMBER

5b. GRANT NUMBER
W81XWH-04-1-0494

5c. PROGRAM ELEMENT NUMBER

6. AUTHOR(S)
Larisa Litovchick, M.D., Ph.D.

E-mail: larisa_litovchick@dfci.harvard.edu

5d. PROJECT NUMBER

5e. TASK NUMBER

5f. WORK UNIT NUMBER

7. PERFORMING ORGANIZATION NAME(S) AND ADDRESS(ES)

Dana Farber Cancer Institute
Boston, MA 02115

8. PERFORMING ORGANIZATION REPORT NUMBER

9. SPONSORING / MONITORING AGENCY NAME(S) AND ADDRESS(ES)
U.S. Army Medical Research and Materiel Command
Fort Detrick, Maryland 21702-5012

10. SPONSOR/MONITOR'S ACRONYM(S)

11. SPONSOR/MONITOR'S REPORT NUMBER(S)

12. DISTRIBUTION / AVAILABILITY STATEMENT
Approved for Public Release; Distribution Unlimited

13. SUPPLEMENTARY NOTES

14. ABSTRACT
The present study was aimed at determining the role of GSK3/RBL2 pathway in rapamycin-mediated growth arrest in prostate cancer cell. Rapamycin and its derivatives are immunosuppressor drugs that also have a potent tumor suppressor effect. These drugs are currently being evaluated in clinical trials to treat human cancers including prostate cancer. Rapamycin exerts its effects through inhibition of mammalian Target of Rapamycin (mTOR) protein kinase resulting in a decreased expression of a subset of proteins essential for cell cycle progression. The cellular pathway mediating cell cycle arrest by rapamycin is still not fully understood. We proposed that Glycogen Synthase Kinase 3 (GSK3) serves as an important mediator of rapamycin effect. Using small-molecule chemical inhibitors of GSK3 and si-RNA depletion, we demonstrated that GSK3 activity is essential for the induction of G0/G1 arrest by rapamycin in prostate cancer (CaP) cell lines LNCaP and PC3. Chemical inhibition of GSK3 prevented accumulation of RBL2/p130 in rapamycin treated cells. RBL2/p130 is an important regulator of G0/G1 in mammalian cells and the lack of RBL2/p130 accumulation could account for the reduced effect of rapamycin in the cells treated with GSK3 inhibitors. Importantly, we also found that a prolonged treatment with GSK3 inhibitors results in cytotoxicity in prostate cancer cells. These findings increase our understanding of the mechanism of the tumor-suppressor effect of rapamycin and set the stage for further evaluation of GSK3 as a potential target for anti-cancer therapy.

15. SUBJECT TERMS
No subject terms provided.

16. SECURITY CLASSIFICATION OF:			**17. LIMITATION OF ABSTRACT**	**18. NUMBER OF PAGES**	**19a. NAME OF RESPONSIBLE PERSON**
					USAMRMC
a. REPORT	**b. ABSTRACT**	**c. THIS PAGE**			**19b. TELEPHONE NUMBER** *(include area code)*
U	U	U	UU	31	

Standard Form 298 (Rev. 8-98)
Prescribed by ANSI Std. Z39.18

Table of Contents

Introduction

Rapamycin is an immunosuppressive agent used in organ transplantation that is also known to inhibit growth of a broad spectrum of tumors, including prostate cancers (CaP) (Sehgal 1998; Hidalgo and Rowinsky 2000; Law 2005). Growth suppression by rapamycin is potent, yet highly cell type-specific. The factors rendering a given tumor sensitive to rapamycin are not yet fully understood, however there is evidence of an increased sensitivity of tumor cells that have lost the function of *PTEN* gene, or have elevated levels of Akt or S6 kinases (Neshat, Mellinghoff et al. 2001; Noh, Mondesire et al. 2004). Mechanistically, rapamycin acts through inhibition of downstream signaling from serine/threonine protein kinase mTOR (Target of Rapamycin), resulting in a decrease of protein synthesis and G1 arrest (Raught, Gingras et al. 2001). The ability of rapamycin to block protein synthesis is in part due to an inhibition of p70 S6 kinase that is phosphorylated and activated by mTOR in the presence of nutrients (Rohde, Heitman et al. 2001). There is a compelling evidence that indicates that TOR is a downstream target of the PI3-K/Akt pathway (Fig. 1) (Fingar and Blenis 2004). Mutations in this pathway such as amplification of *PI3-K* and *AKT*, or loss of *PTEN* genes result in an activated state of the pathway and are important for cancer progression (McMenamin, Soung et al. 1999; Nakatani, Thompson et al. 1999; Kwabi-Addo, Giri et al. 2001; Murillo, Huang et al. 2001).

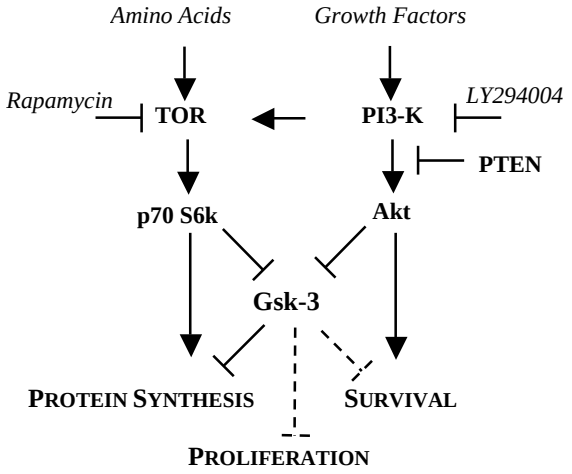

Fig. 1. Panel A: PI3-K/TOR pathway and Glycogen-Synthase Kinase-3 (GSK3). Amino acids and growth factors activate TOR and PI3-K, which in turn activate downstream partners such as p70 S6k and Akt. These kinases then phosphorylate multiple targets responsible for an increased protein synthesis and cell survival. Importantly, both p70 S6k and Akt phosphorylate and inhibit GSK3, a multifunctional kinase that has been implicated into the control of diverse processes including glycogen and protein synthesis, early embryonic development and possibly cell survival and proliferation (Woodgett 2001).

The retinoblastoma (Rb) family, including pRb, Rbl1/p107 and Rbl2/p130 is indispensable for the ability of mammalian cells to enter the G1/G0 growth arrested state and is often inactivated in cancer (Smith, Leone et al. 1996. Unlike pRB and p107, p130 is specifically phosphorylated in G0/G1 arrested cells {Hansen, 2001 #103; Canhoto, Chestukhin et al. 2000; Classon,

Salama et al. 2000; Dannenberg, van Rossum et al. 2000; Farkas, Hansen et al. 2002; Litovchick, Chestukhin et al. 2004).

We found that p130 is phosphorylated by GSK3 *in vivo* in G0/G1 arrested cells and mapped the three sites phosphorylated by GSK3 in p130 to the unique region that is not present in pRB or p107 (Litovchick, Chestukhin et al. 2004). This phosphorylation could be relevant to the effects mediated by PI3-K/AKT/mTOR pathway, because GSK3 is phosphorylated and inhibited by both p70 S6k and AKT (Fig.1) (Woodgett 2001). Unlike most protein kinases involved into PI3-K/AKT signaling, GSK3 is inhibited upon activation of this pathway and therefore GSK3 could be activated by rapamycin. Phosphorylation of RBL2/p130 by GSK3 regulated by the PI3-K/AKT/mTOR pathway represents a previously untested link in the molecular pathway targeted by rapamycin that could be critical for its growth suppression effect. When our study was being finalized, another group also reported that GSK3 is an important contributor to the growth suppression effect of rapamycin, possibly by decreasing the stability of cyclin D1 (Dong, Peng et al. 2005).

Objectives:

The present Exploration: Hypothesis Development study was designed to achieve the following specific aims:

Aim 1. To establish whether Gsk-3 is an important mediator of the rapamycin-induced growth arrest in prostate cancer cells.

Aim 2. To determine the role of Gsk-3 phosphorylation of Rbl2/p130 in rapamycin-induced G1 arrest in prostate cancer cells.

Here we report that that GSK3 activity is essential for the induction of G0/G1 arrest by Rapamycin in prostate cancer (CaP) cell lines LNCaP and PC3. Chemical inhibition of GSK3 prevented accumulation of RBL2/p130 in rapamycin treated cells. RBL2/p130 is an important regulator of G0/G1 in mammalian cells and the lack of RBL2/p130 accumulation could account for the reduced growth suppressing effect of rapamycin in the cells treated with GSK3 inhibitors. Importantly, we have also found that a prolonged treatment with GSK3 inhibitors results in cytotoxicity in prostate cancer cells. These findings increase our understanding of the mechanism of the rapamycin effects and set the stage for further evaluation of GSK3 as a potential target for anti-cancer therapy for prostate cancer and other types of human cancer.

Report Body

Rapamycin treatment of CaP cells induces up-regulation of p130 but not pRB or p107.

We have recently demonstrated that RBL2/p130 is phosphorylated by GSK3 in G0/G1 arrested cells and that GSK3 phosphorylation increased stability of p130 (Litovchick, Chestukhin et al. 2004). Given that GSK3 is negatively regulated by mTOR pathway (Fig. 1 and (Woodgett 2001)), we hypothesized that rapamycin can affect levels of p130 via GSK3. To test this hypothesis, we treated several prostate cancer cell lines (DU145, PC3 and LNCaP) with rapamycin and monitored expression of p130 by Western blot analysis (Fig. 2A). Indeed, we observed a significant increase in p130 expression levels in all tested cell lines upon rapamycin treatment. In the same experiment, we have also looked into expression levels of other RB family members (Fig. 2A). Expression of p107 and was decreased (PC3 and LNCaP) or unchanged (DU145) upon the treatment, while levels of pRB were also decreased in all lines that express pRB. The cellular effects of rapamycin include inhibition of protein synthesis and cell growth as well as G1 arrest (Rohde, Heitman et al. 2001). We compared the cell cycle profile of control and rapamycin treated cell lines by FACS analysis and observed an increase of G0/G1 cell population in rapamycin treated cells. PC3 and LNCaP cells exhibited a dramatic response to rapamycin while DU145 cells displayed less prominent response (Fig. 2A). This observation is in agreement with previously reported elevated sensitivity of the *PTEN* negative cell lines (PC3, LNCaP) compared to wild type *PTEN* cells (DU145) (Neshat, Mellinghoff et al. 2001). Since p130 was up-regulated in all tested cell lines upon rapamycin treatment, we concluded that accumulation of p130 does not depend on *PTEN* status of the CaP cells.

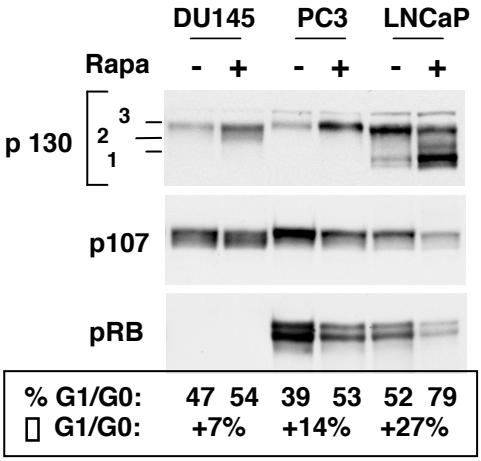

Fig. 2A. The effect of rapamycin on RB family in CaP cell lines. The indicated cell lines were incubated for 24 h in a complete growth medium in the absence (-) or in the presence (+) of 50 nM rapamycin. Expression of RB family proteins was then analyzed by Western blot with specific antibodies. Note an increase of p130 levels upon the rapamycin treatment. In the same experiment, cell cycle profiles were analyzed by FACS analysis of DNA content. The changes in G1/G0 cell population are shown at the bottom of the figure.

LNCaP cells displayed most dramatic increase in G0/G1 cell population as well as most significant accumulation of hypo-phosphorylated forms of p130 (bands 1 and 2, Fig. 2A) upon rapamycin treatment as compared with DU145 and PC3. We have previously demonstrated that GSK3 phosphorylation contributes to formation of hypo-phosphorylated forms of p130

(Litovchick, Chestukhin et al. 2004) and therefore we wanted to test whether GSK3 activity is essential for accumulation of p130 upon rapamycin treatment. To do so, we downregulated GSK3 activity by siRNA depletion of GSK3 and isoforms as well as by chemical inhibition of GSK3 using LiCl and small molecule inhibitor I-8 (Ryves and Harwood 2001; Bhat, Xue et al. 2003).

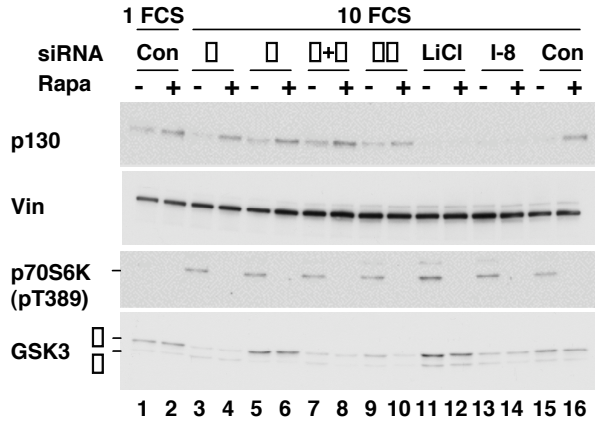

Fig. 2B. The effect of GSK3 inhibition on the accumulation of p130 induced by rapamycin in DU145 cells. DU145 were transfected with siRNA duplexes specific to human GSK3, GSK3, a mixture of the two, a siRNA duplex targeting both GSK3 and or a control non-targeting siRNA, as indicated. The cell were incubated in a growth medium containing 1% FCS for 24 h after transfection before changing into the medium containing 10% FCS. The drugs (rapamycin, 100 nM; LiCl, 25 mM (Ryves and Harwood 2001) and I-8, 30 M (Bhat, Xue et al. 2003)) were added at the same time and incubated for additional 24 h before collecting the cell extracts for Western blot analysis with indicated antibodies. One of the control-transfected series was left in the low-serum medium for 48 h after transfection to determine basal levels of p70S6K phosphorylation (**1 FCS**). Vinculin blot is shown as a loading control.

As seen in Fig. 2B, the levels of p130 were decreased in the cells incubated with 10% FCS (compare lanes 1 and 15). Treatment with rapamycin resulted in increase of p130 levels (compare lanes 15 and 16). Addition of either LiCl or GSK3 inhibitor I-8 prevented accumulation of p130 upon rapamycin treatment (lanes 11 – 14). GSK3 inhibitors did not affect mTOR signaling as evident from unchanged levels of phosphorylation of mTOR target p70S6K on Thr389. The siRNA depletion of GSK3 or isoforms or both did not affect accumulation of p130 upon rapamycin treatment, probably because of incomplete depletion of GSK3 achieved in this experiment (Fig. 2B, lanes 3 – 10). We chose to present here the experiment performed in DU145 CaP cell because we were able to achieve the most significant depletion of GSK3 by siRNA transfection in these cells (Fig. 2B). Treatment with LiCl or chemical GSK3 inhibitors of several other human cancer cell lines also resulted in down-regulation of p130 protein levels and blocked accumulation of p130 upon rapamycin treatment or serum starvation (data not shown).

Inhibition of GSK3 selectively reduces G1 arrest by rapamycin in CaP cells.

We have previously demonstrated that GSK3 phosphorylation contributes to formation of hypo-phosphorylated forms of p130 (Litovchick, Chestukhin et al. 2004) and therefore we tested whether GSK3 activity is essential for induction of G1 arrest upon rapamycin treatment. To do so, we used specific inhibitors of GSK3 including LiCl (Ryves and Harwood 2001), as well as recently released small molecule inhibitors I-8 and I-9 (Bhat, Xue et al. 2003; Sato, Meijer et al.

2004). Both I-8 and I-9 have been shown to inhibit GSK3 in cultured cells in the micromolar concentration range. To quantitatively access the effect of rapamycin and GSK3 inhibitors on the cell cycle, we analyzed DNA synthesis of the rapamycin-treated cells using BRDU incorporation assay followed by FACS analysis.

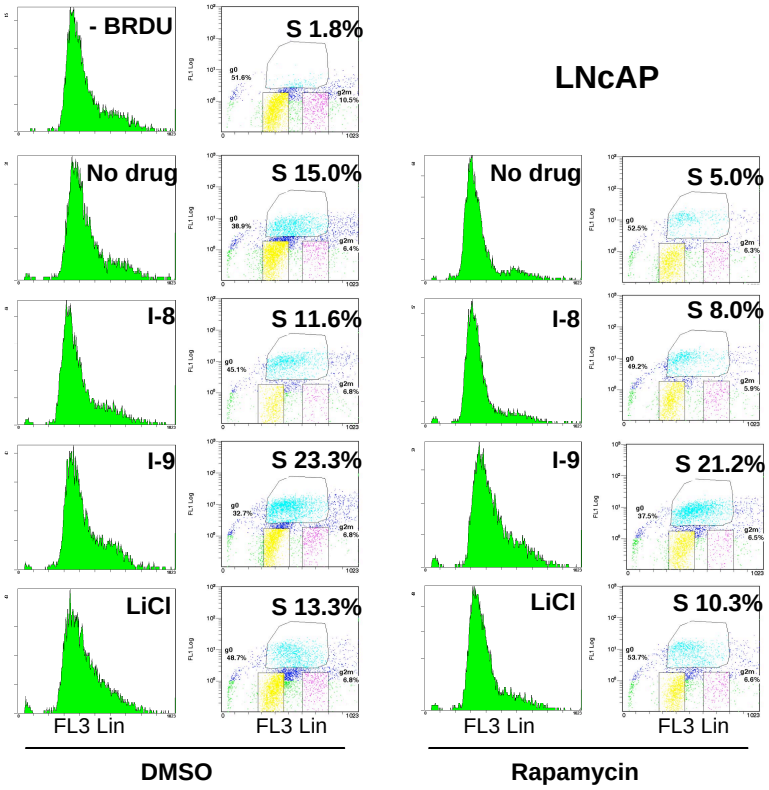

Fig. 3A. The effect of GSK3 inhibition on rapamycin-induced cell cycle arrest in LNCaP cells. LNCaP cells (50% confluent) were incubated for 24h in the complete growth medium containing no drugs, 10 □M I-8, 3 □M I-9 or 12.5 mM LiCl, in the absence (DMSO) or in the presence of 100 nM rapamycin. The cells were then incubated with BRDU for 30 min and the percentage of cells in S-phase was then determined by FACS analysis using FITC-labeled anti-BRDU antibody. Percent of cells in S-phase was calculated by measuring BRDU-positive cells. The cells incubated without any drugs or BRDU were stained with anti-BRDU antibody and serve as a negative control (Top left graph, **-BRDU**). Total DNA content was simultaneously analyzed using PI staining (histograms on the left panels).

We observed a significant decrease in DNA-synthesizing population of LNCaP cells after treatment with rapamycin (from 15% to 5%) (Fig. 3A, no drug series). Treatment of the cells with I-8 or LiCl resulted in less prominent decrease in BRDU-positive cell population (from 11.6% to 8% and from 13.3% to 10.3%, respectively). Interestingly, while both I-8 and LiCl induced a slight reduction in DNA synthesizing population of DMSO-treated LNCaP cells, treatment with I-9 resulted in the increased BRDU incorporation that was essentially unaffected by rapamycin treatment (control, 23.3% and rapamycin, 21.2%) (Fig. 3A). While it is unclear why some GSK3 inhibitors (I-8 and LiCl) were able to slightly inhibit DNA synthesis and other (I-9) appear to stimulate DNA synthesis, this experiment suggests that all GSK3-targeting drugs significantly deceased cell cycle inhibitory effect of rapamycin in LNCaP cells.

To address the cell type-specific effects of the treatments, we repeated the same experiment using another highly rapamycin sensitive CaP cell line, PC3 (Fig. 3B).

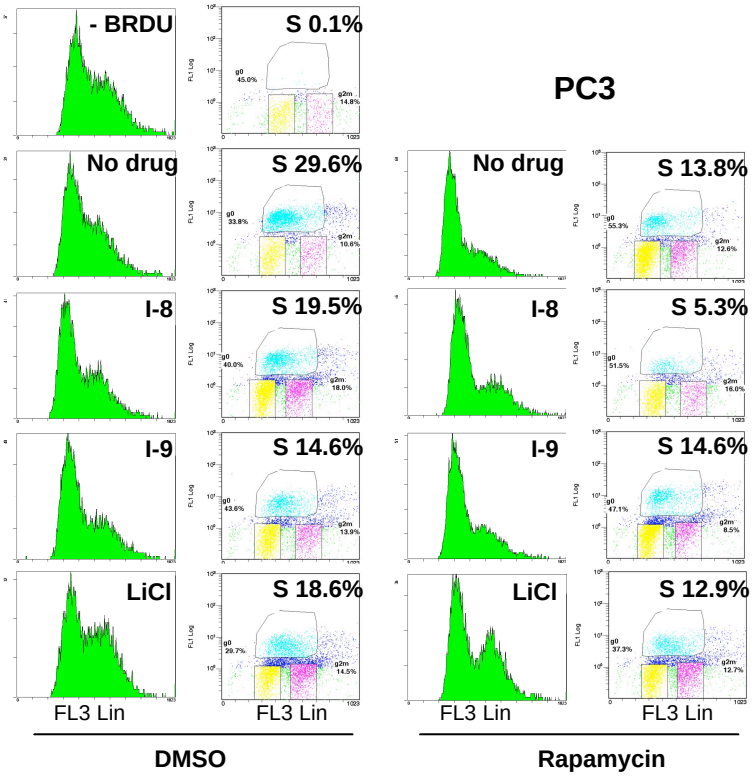

Fig. 3B. The effect of GSK3 inhibition on rapamycin-induced cell cycle arrest in PC3 cells. PC3 cells (30% confluent) were incubated for 24h in the complete growth medium containing no drugs, 10 μM I-8, 3 μM I-9 or 12.5 mM LiCl, in the absence (DMSO) or in the presence of 100 nM rapamycin. The cells were labeled with BRDU and assayed as described in legend for Fig.3A.

As expected, rapamycin treatment of PC3 cells induced a dramatic reduction of the BRDU-positive cell population (from 29.6% to 13.8%) (Fig. 3B). Incubation of GSK3 inhibitory drugs alone reduced the percentage of DNA-synthesizing PC3 cells (no drugs, 29.6%; I-8, 19.5%; I-9, 14.6% and LiCl, 18.6%). Rapamycin treatment was able to further dramatically reduce this population in the presence of I-8 (from 19.5% to 5.3%) and also in the presence of LiCl (from 18.6% to 12.9%) but not in the presence of I-9 (14.6%, unchanged).

Therefore, it appears that while there is an indication of the antagonistic effect between GSK3 inhibitors and rapamycin with respect to the cell cycle arrest, there is a significant cell-type specific variation in the response of the cells to GSK3 inhibition, both with and without rapamycin treatment. More studies are necessary to determine whether the observed effects are indeed specific to GSK3. While the LiCl is the most widely used GSK3 inhibitor, it could potentially inhibit other cellular kinases such as CK2 and MAPKAP-K2 (Davies, Reddy et al. 2000). The new generation inhibitors, I-8 and I-9 are expected to be more specific towards GSK3 but there is not enough data yet to demonstrate this specificity. In our experiments described above, there seem to be a difference between the effects of different GSK3 inhibitors on a given CaP cell line. While both I-8 and LiCl induce mostly similar responses, I-9 stands apart, possibly because of some additional targets affected by this compound. In course of this study, we attempted small interference RNA depletion of GSK3 in LNCaP and PC3 cells in order to support or disprove our data on GSK3 inhibitors. Although we were able to achieve a partial reduction in GSK3 levels using transient transfection of GSK3 and GSK3 –specific siRNA duplexes (obtained from Dharmacon and Cell Signaling Technology), the resulting GSK3 down-regulation was not sufficient to recapitulate biological effects similar to that induced by

chemical inhibitors of GSK3 (data not shown). Similarly, the ectopic expression of kinase-dead allele of GSK3b was not sufficient to reproduce these effects (data not shown).

Effect of GSK3 inhibitors on the tumor suppression by rapamycin.

Rapamycin has been shown to inhibit proliferation of a broad range of human cancer cell types and to slow down tumor progression *in vivo* (Law 2005). This effect of rapamycin could be in part dependent on the ability of rapamycin to induce G0/G1 cell cycle arrest. Since our data described above indicate that GSK3 activity is essential for G1 arrest induction by rapamycin, we tested whether inhibition of GSK3 could antagonize anti-proliferative effect of rapamycin on CaP cells. We performed cell proliferation assay using CaP cell lines LNCaP, PC3 and DU145 treated with 30 or 100 nM of rapamycin combined with inhibitors of GSK3 (LiCl, I-8 and I-9). GSK3 inhibitors were used in concentrations previously used by other groups to inhibit GSK3 activity under similar experimental conditions (Ryves and Harwood 2001; Bhat, Xue et al. 2003; Sato, Meijer et al. 2004). We have also established that these concentrations of GSK3 inhibitors were sufficient to block GSK3-induced phosphorylation of p130 in T98G human glioblastoma cells (data not shown).

As shown in Fig. 4, treatment with 30 and 100 nM rapamycin reduced cell density of LNCaP cells to 60 and 50% of control, respectively (DMSO and KCl series). The cell density of LNCaP series treated with LiCl or I-8 was decreased even in the absence of rapamycin. However, rapamycin treatment was able to further reduce the cell density, indicating that neither LiCl nor I-8 were able to antagonize growth suppression by rapamycin (Fig. 4B). Treatment with I-9, however, appeared to reduce the efficiency of rapamycin growth suppression. This result is in a good agreement with the data described above when I-9 treatment was shown to reduce the rapamycin-induced cell cycle arrest in LNCaP cells (Fig. 3).

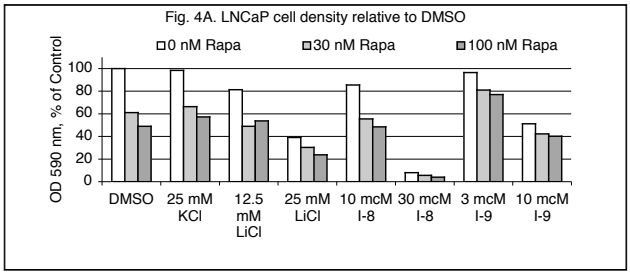

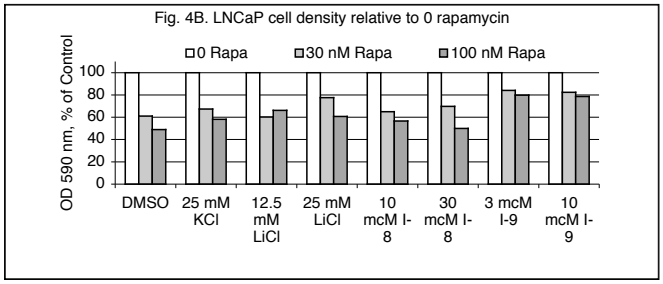

Fig. 4. The effect of GSK3 inhibitors on growth suppression by rapamycin in LNCaP cells. LNCaP cells were seeded in a complete growth medium on 6-well plates (30% confluent) and allowed to attach overnight. The cell were then treated with indicated concentrations of rapamycin and GSK3 inhibitors for 3 days before determining the cell density using crystal violet assay (Dannenberg, van Rossum et al. 2000). DMSO (0.1%) and KCl (25 mM) serve as controls. **Panel A** shows the relative cell density values expressed as a percent of that of the series with no drug treatment (0 Rapa, DMSO). Panel B shows the cell density values in each GSK3 inhibitor drug series relative to the cell density of "0 Rapa" sample in the same series. Representative results of 3 similar experiments are shown.

Interestingly, the effect of GSK3 inhibitor I-9 was even more dramatic in PC3 cells where both 3 and 10 μM concentrations of I-9 were able to abrogate the anti-proliferative effect of rapamycin on PC3 cells (Fig. 5A, compare DMSO series and I-9 series). Moreover, incubation of the cells in the presence of 3 μM of I-9 resulted in an increased cell density compared to control DMSO series (140%). Addition of 10 μM of I-8 also resulted in increased cell density in this series (Fig. 5A) but did not affect the effect of rapamycin (better seen in Fig. 5B), while 30 μM concentration of I-8 abrogated the effect of rapamycin (Fig. 5B) but also resulted in significantly decreased cell densities in this series (Fig. 5A). Conversely, LiCl treatment appeared to slightly increase the sensitivity of PC3 cells to rapamycin (Fig. 5B) although the cell density was reduced in the presence of 25 mM LiCl (Fig. 5A). Importantly, unlike rapamycin that only suppressed the proliferation of CaP cells in this assay but did not induce the cell death, GSK3 inhibitors treatment resulted in CaP cell death as judged by an increased numbers of detached non-viable cells accumulating upon GSK3 inhibitors treatment.

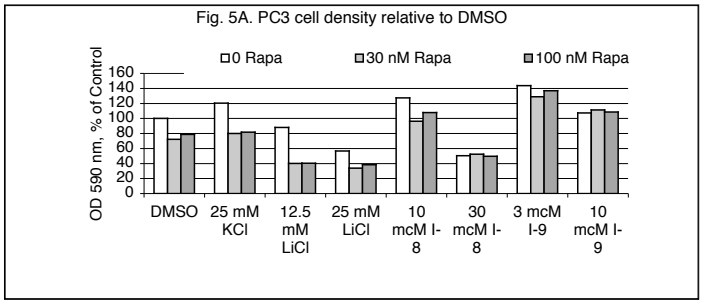

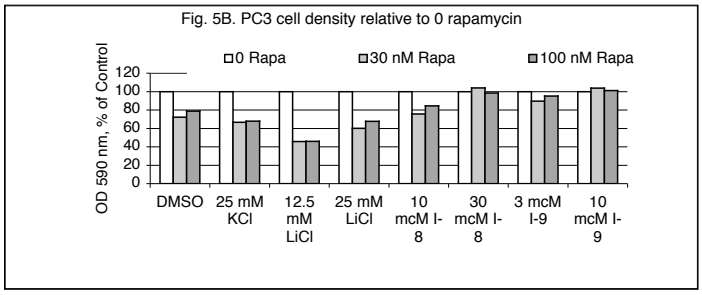

Fig. 5. The effect of GSK3 inhibitors on growth suppression by rapamycin in PC3 cells. PC3 cells were seeded in a complete growth medium on 6-well plates (30% confluent) and allowed to attach overnight. The cell were then treated with indicated concentrations of rapamycin and GSK3 inhibitors for 3 days before determining the cell density using crystal violet assay (Dannenberg, van Rossum et al. 2000). DMSO (0.1%) and KCl (25 mM) serve as controls. **Panel A** shows the relative cell density values expressed as a percent of that of the series with no drug treatment (0 Rapa, DMSO). Panel B shows the cell density values in each GSK3 inhibitor drug series relative to the cell density of "0 Rapa" sample in the same series. Representative results are shown.

Conclusions

The data presented above suggests that GSK3 activity is essential for both growth suppression and the cell cycle arrest effects of rapamycin in CaP cells. GSK3 inhibitor I-9 was able to dramatically decrease both G1 arrest and growth inhibitory effects of rapamycin in highly rapamycin-sensitive CaP cell lines, LNCaP and PC3. GSK3 inhibitor I-8 appeared less potent in these experiments but it was also able to block the growth suppressing effect of rapamycin in 30 M concentration in PC3 cells. These effects of GSK3 inhibitors could be attributed to the fact that GSK3 inhibitors blocked accumulation of RBL2/p130, an important regulator of G1/G0 checkpoint. At the present level of knowledge, it is difficult to explain why various GSK3 inhibitors including LiCl, I-8 and I-9 induce such different cellular responses when used alone or in combination with rapamycin. Cell lines could have different intrinsic sensitivities to these drugs or GSK3 inhibitors could affect other cellular pathways independently of GSK3 inhibition. Finally, we observed a significant cytotoxic effect of GSK3 inhibitors in cell growth assays in LNCaP and PC3 cells. This result is somewhat unexpected given a recognized role of GSK3 in induction of apoptosis (Bijur, De Sarno et al. 2000; Hetman, Cavanaugh et al. 2000), but it is in agreement with a finding that an acute ablation of GSK3 activity induces apoptosis in colon cancer cells recently published by another group (Ghosh and Altieri 2005). Although the interest to GSK3 dramatically increased during past few years, its role in cell cycle progression, cell survival and cancer remains controversial. Our results presented here show that while GSK3 is an important contributor to the tumor suppression effect of rapamycin, this kinase can also contribute to prostate cancer survival. Further studies are needed to understand the function and regulation of GSK3 in normal and cancer cells.

Key Research Accomplishments

(During the period covered by EHD Award in Prostate Cancer Research from Department of Defense to Dr. Larisa Litovchick, M.D., Ph.D.)

- **Research article:**

Litovchick, L., A. Chestukhin, and J. DeCaprio. (2004). "Glycogen synthase kinase 3 phosphorylates RBL2/p130 during quiescence." Mol Cell Biol **24**(20): 8970-80.

- **Conference proceedings:**

Chestukhin, A., Litovchick, L., DeCaprio, J., ASBMB Annual Meeting and 8th IUBMB Conference, June 12 - 16, 2004, “Cell cycle dependent regulation of separase expression and localization” (Abstract).

Litovchick, L., Chestukhin, A., DeCaprio, J., ASBMB Annual Meeting and 8th IUBMB Conference, June 12 - 16, 2004, “The role of Glycogen Synthase Kinase-3 in cell cycle control by RBL2/p130”.

Reportable Outcomes

- The EHD Award from Department of Defense, Prostate Cancer Research Program, served as grounds for Principal Investigator Dr. Larisa Litovchick, M.D., Ph.D., to apply for a promotion at Harvard Medical School, Boston, MA. Promotion to an **Instructor in Medicine** was granted in November 2004.
- Findings and concepts emanated from this study were used to apply for **Eleanor and Miles Shore Scholars in Medicine Fellowships Program, Dana-Farber Cancer Institute Fellowship** (funding started in August 2004);
- Findings and concepts emanated from this study were used to apply for **Raising Stars Fellowship, Dunkin Doughnuts sponsored Dana-Farber Cancer Institute Career Development Fellowship** (not funded);
- Findings and concepts obtained in this study will be used to apply for **Prostate Cancer SPORE Fellowship, Dana-Farber Cancer Institute** (application deadline November 30, 2005);

References

Bhat, R., Y. Xue, et al. (2003). "Structural insights and biological effects of glycogen synthase kinase 3-specific inhibitor AR-A014418." J Biol Chem **278**(46): 45937-45.

Bijur, G. N., P. De Sarno, et al. (2000). "Glycogen synthase kinase-3beta facilitates staurosporine- and heat shock-induced apoptosis. Protection by lithium." J Biol Chem **275**(11): 7583-90.

Canhoto, A. J., A. Chestukhin, et al. (2000). "Phosphorylation of the retinoblastoma-related protein p130 in growth-arrested cells." Oncogene **19**(44): 5116-22.

Classon, M., S. Salama, et al. (2000). "Combinatorial roles for pRB, p107, and p130 in E2F-mediated cell cycle control." Proceedings of the National Academy of Sciences of the United States of America **97**(20): 10820-5.

Dannenberg, J. H., A. van Rossum, et al. (2000). "Ablation of the retinoblastoma gene family deregulates G(1) control causing immortalization and increased cell turnover under growth-restricting conditions." Genes Dev **14**(23): 3051-64.

Davies, S. P., H. Reddy, et al. (2000). "Specificity and mechanism of action of some commonly used protein kinase inhibitors." Biochem J **351**(Pt 1): 95-105.

Dong, J., J. Peng, et al. (2005). "Role of glycogen synthase kinase 3beta in rapamycin-mediated cell cycle regulation and chemosensitivity." Cancer Res **65**(5): 1961-72.

Farkas, T., K. Hansen, et al. (2002). "Distinct phosphorylation events regulate p130- and p107-mediated repression of E2F-4." J Biol Chem **277**(30): 26741-52.

Fingar, D. C. and J. Blenis (2004). "Target of rapamycin (TOR): an integrator of nutrient and growth factor signals and coordinator of cell growth and cell cycle progression." Oncogene **23**(18): 3151-71.

Ghosh, J. C. and D. C. Altieri (2005). "Activation of p53-dependent apoptosis by acute ablation of glycogen synthase kinase-3beta in colorectal cancer cells." Clin Cancer Res **11**(12): 4580-8.

Hetman, M., J. E. Cavanaugh, et al. (2000). "Role of glycogen synthase kinase-3beta in neuronal apoptosis induced by trophic withdrawal." J Neurosci **20**(7): 2567-74.

Hidalgo, M. and E. K. Rowinsky (2000). "The rapamycin-sensitive signal transduction pathway as a target for cancer therapy." Oncogene **19**(56): 6680-6.

Kwabi-Addo, B., D. Giri, et al. (2001). "Haploinsufficiency of the Pten tumor suppressor gene promotes prostate cancer progression." Proc Natl Acad Sci U S A **98**(20): 11563-8.

Law, B. K. (2005). "Rapamycin: an anti-cancer immunosuppressant?" Crit Rev Oncol Hematol **56**(1): 47-60.

Litovchick, L., A. Chestukhin, et al. (2004). "Glycogen synthase kinase 3 phosphorylates RBL2/p130 during quiescence." Mol Cell Biol **24**(20): 8970-80.

McMenamin, M. E., P. Soung, et al. (1999). "Loss of PTEN expression in paraffin-embedded primary prostate cancer correlates with high Gleason score and advanced stage." Cancer Res **59**(17): 4291-6.

Murillo, H., H. Huang, et al. (2001). "Role of PI3K signaling in survival and progression of LNCaP prostate cancer cells to the androgen refractory state." Endocrinology **142**(11): 4795-805.

Nakatani, K., D. A. Thompson, et al. (1999). "Up-regulation of Akt3 in estrogen receptor-deficient breast cancers and androgen-independent prostate cancer lines." J Biol Chem **274**(31): 21528-32.

Neshat, M. S., I. K. Mellinghoff, et al. (2001). "Enhanced sensitivity of PTEN-deficient tumors to inhibition of FRAP/mTOR." Proc Natl Acad Sci U S A **98**(18): 10314-9.

Noh, W. C., W. H. Mondesire, et al. (2004). "Determinants of rapamycin sensitivity in breast cancer cells." Clin Cancer Res **10**(3): 1013-23.

Raught, B., A. C. Gingras, et al. (2001). "The target of rapamycin (TOR) proteins." Proc Natl Acad Sci U S A **98**(13): 7037-44.

Rohde, J., J. Heitman, et al. (2001). "The TOR kinases link nutrient sensing to cell growth." J Biol Chem **276**(13): 9583-6.

Ryves, W. J. and A. J. Harwood (2001). "Lithium inhibits glycogen synthase kinase-3 by competition for magnesium." Biochem Biophys Res Commun **280**(3): 720-5.

Sato, N., L. Meijer, et al. (2004). "Maintenance of pluripotency in human and mouse embryonic stem cells through activation of Wnt signaling by a pharmacological GSK-3-specific inhibitor." Nat Med **10**(1): 55-63.

Sehgal, S. N. (1998). "Rapamune (RAPA, rapamycin, sirolimus): mechanism of action immunosuppressive effect results from blockade of signal transduction and inhibition of cell cycle progression." Clin Biochem **31**(5): 335-40.

Smith, E. J., G. Leone, et al. (1996). "The accumulation of an E2F-p130 transcriptional repressor distinguishes a G0 cell state from a G1 cell state." Molecular & Cellular Biology **16**(12): 6965-76.

Woodgett, J. R. (2001). "Judging a protein by more than its name: GSK-3." Sci STKE **2001**(100): RE12.

Abbreviations

BRDU - Bromodeoxyuridine

CaP – Prostate cancer
FACS – Fluorescence activated cell scanning
FCS – Fetal clone serum
GSK3 – Glycogen Synthase Kinase 3
mTOR – mammalian Target of Rapamycin
PI – Propidium Iodide

Methods

Reagents. Rapamycin, GSK3 I-8 (AR-A014418, N-(4-Methoxybenzyl)-N'-(5-nitro-1,3-thiazol-2-yl)urea) and GSK3 I-9 (BIO, (2' *Z*,3' *E*)-6-Bromoindirubin-3'-oxime) were purchased from Calbiochem and dissolved in DMSO. Cell proliferation labeling reagent (BRDU) was purchased from Amersham Pharmacia Biotech. FITC-conjugated BRDU detection monoclonal antibody kit was from BD Pharmingen. Propidium Iodide and Crystal Violet were from Sigma. Antibodies were from the following sources: rabbit anti-p130 (C-20) and p107 (C-18) antibodies were from Santa Cruz, mouse anti-Rb antibody was from BD Pharmingen, rabbit anti-pThr398 p70S6K antibodies were from Cell Signaling Technology, mouse anti-GSK3 antibody was from UBI and mouse anti-vinculin antibody was from Sigma.

Cell lines and treatments. DU145, LNCaP and PC3 cells were from ATCC. The cells were tested for mycoplasma contamination and confirmed mycoplasma free using Mycodetect PCR kit (Stratagene). DU145 and LNCaP cells were cultured in RPMI (Gibco) supplemented with 10% FCS and standard antibiotic mixture. PC3 cells were cultured in Ham's F12 medium (Gibco) supplemented with 10% FCS and standard antibiotic mixture. The cells were treated with various drugs added directly to the culture medium from DMSO stock solutions and incubated as described in Figure legends. The cells treated with appropriate amount of DMSO served as a negative control. For Western blot analysis, the cells were extracted with SDS-PAGE loading buffer containing no loading dye. The protein concentration was determined using Dc Protein Assay kit (Bio-Rad). For cell cycle analysis, the cell proliferation labeling reagent was added directly to the cell culture medium and the cells were collected by trypsinization 30 min later. The cells were then washed with PBS and fixed in 70% ethanol. The staining of the cells with FITC-anti BRDU antibody and PI was then performed according to the kit manufacturers instructions. The samples were analyzed using FC500 Analyzer (Beckman Coulter). For cell growth assays, the cells were plated onto 6-well plates at 30% confluency and treated as described in Figure legends. The cells were then stained with Crystal Violet dye according to the manufacturers instructions, washed with distilled water, dried and then the absorbed dye was solubilized using 10% acetic acid. The optical density of samples was then determined by spectrophotometer at 590 nm.

Appendices.

1. Updated Curriculum Vitae, Larisa Litovchick, M.D., Ph.D.

2. Manuscript "Glycogen synthase kinase 3 phosphorylates RBL2/p130 during quiescence" by **Litovchick L**, A. Chestukhin, and J. A. DeCaprio. Mol Cell Biol 2004; 24(20):8970-80.

CURRICULUM VITAE

Date Prepared:	10/05
Name:	Larisa Litovchick
Office Address:	Dana-Farber Cancer Institute, 44 Binney Street, Mayer 444, Boston, MA 02115
E-mail:	larisa_litovchick@dfci.harvard.edu
Phone:	617-632-5715
Fax:	617-632-4760

Education:

1993	M.Sc.	Biophysics, Department of Biophysics, The Russian Medical University, Moscow, Russia
1993	M.D.	Bio-Medical Faculty, The Russian Medical University, Moscow, Russia
2000	Ph.D.	Life Sciences Department, The Weizmann Institute of Science, Rehovot, Israel

Experience:

1991-1993	Undergraduate Student, Laboratory of the Chemical Basis of Biocatalysis, Engelgardt Institute of Molecular Biology, Moscow, Russia (Alexander G. Gabibov, Ph.D., Principal Investigator)
1993-1994	Visiting Student, Chemical Immunology Department, Weizmann Institute of Science, Rehovot, Israel (Professor Shmuel Shaltiel, Ph.D., Principal Investigator)
1994-1999	Graduate Student, Department of Biological Regulation, Weizmann Institute of Science, Rehovot, Israel (Professor Shmuel Shaltiel, Ph.D., Principal Investigator)
1999-	Research Associate in Medicine, Department of Medical Oncology, Dana-Farber Cancer Institute, Boston, MA (James A. DeCaprio, M.D., Principal Investigator)
1999-2004	Research Fellow in Medicine, Department of Medicine, Harvard Medical School, Boston, MA
2004-	Instructor in Medicine, Harvard Medical School, Boston, MA

Awards:

2003- Exploration: Hypothesis Development Award, Department of Defense, Congressionally Directed Medical Research Programs, Prostate Cancer Research Program.

2004- Eleanor and Miles Shore Scholars in Medicine Fellowships Program, Dana-Farber Cancer Institute Fellowship.

BIBLIOGRAPHY

Original Reports

1. **Litovchick L**, Aleksandrova E S, Gabibov AG, and Bronshtein IB. Interaction of camptothecin with topoisomerase I studied by fluorescence spectroscopy Dokl Akad Nauk 1995; 340 (2): 271-2

2. Chestukhin, A., **L. Litovchick**, M. Batkin, and S. Shaltiel. Anti-head and anti-tail antibodies against distinct epitopes in the catalytic subunit of protein kinase A. Use in the study of the kinase splitting membranal proteinase KSMP. FEBS Lett 1996; 382:265-70.

3. Chestukhin, A., **L. Litovchick**, D. Schourov, S. Cox, S. S. Taylor, and S. Shaltiel. Functional malleability of the carboxyl-terminal tail in protein kinase A. J Biol Chem 1996; 271:10175-82.

4. Chestukhin, A., K. Muradov, **L. Litovchick**, and S. Shaltiel. The cleavage of protein kinase A by the kinase-splitting membranal proteinase is reproduced by meprin beta. J Biol Chem 1996; 271:30272-80.

5. Chestukhin, A.*, **L. Litovchick***, K. Muradov, M. Batkin, and S. Shaltiel. Unveiling the substrate specificity of meprin beta on the basis of the site in protein kinase A cleaved by the kinase splitting membranal proteinase. J Biol Chem 1997; 272:3153-60.

6. Canhoto, A. J., A. Chestukhin, **L. Litovchick**, and J. A. DeCaprio. Phosphorylation of the retinoblastoma-related protein p130 in growth-arrested cells. Oncogene 2000; 19:5116-22.

7. Chestukhin, A., **L. Litovchick**, K. Rudich, and J. A. DeCaprio. Nucleocytoplasmic shuttling of p130/RBL2: novel regulatory mechanism. Mol Cell Biol 2002; 22:453-68.

8. **Litovchick, L**., A. Chestukhin, and S. Shaltiel. The carboxyl-terminal tail of kinase splitting membranal proteinase/meprin beta is involved in its intracellular trafficking. J Biol Chem 1998; 273:29043-51.

9. **Litovchick, L**., E. Friedmann, and S. Shaltiel. A selective interaction between OS-9 and the carboxyl-terminal tail of meprin beta. J Biol Chem 2002; 277:34413-23.

10. **Litovchick L**, A. Chestukhin, and J. A. DeCaprio. Glycogen synthase kinase 3 phosphorylates RBL2/p130 during quiescence. Mol Cell Biol 2004; 24(20):8970-80.

* - Authors equally contributed to the manuscript.

MOLECULAR AND CELLULAR BIOLOGY, Oct. 2004, p. 8970–8980 Vol. 24, No. 20
0270-7306/04/$08.00+0 DOI: 10.1128/MCB.24.20.8970–8980.2004

Glycogen Synthase Kinase 3 Phosphorylates RBL2/p130 during Quiescence

Larisa Litovchick, Anton Chestukhin, and James A. DeCaprio*

Dana-Farber Cancer Institute, Boston, Massachusetts

Received 11 May 2004/Returned for modification 9 June 2004/Accepted 22 July 2004

Phosphorylation of the retinoblastoma-related or pocket proteins RB1/pRb, RBL1/p107, and RBL2/p130 regulates cell cycle progression and exit. While all pocket proteins are phosphorylated by cyclin-dependent kinases (CDKs) during the G_1/S-phase transition, p130 is also specifically phosphorylated in G_0-arrested cells. We have previously identified several phosphorylated residues that match the consensus site for glycogen synthase kinase 3 (GSK3) in the G_0 form of p130. Using small-molecule inhibitors of GSK3, site-specific mutants of p130, and phospho-specific antibodies, we demonstrate here that GSK3 phosphorylates p130 during G_0. Phosphorylation of p130 by GSK3 contributes to the stability of p130 but does not affect its ability to interact with E2F4 or cyclins. Regulation of p130 by GSK3 provides a novel link between growth factor signaling and regulation of the cell cycle progression and exit.

Control of the cell cycle relies on the precisely regulated expression of the genes required for the cell cycle progression. The pocket proteins, including RB1/pRb, RBL1/p107, and RBL2/pRb2/p130, play overlapping but distinct roles in the regulation of the cell cycle (6, 7, 36). pRb, p107, and p130 share significant homology with each other, especially in two domains (A and B; see Fig. 1A) that together form the pocket domain critical for interaction with E2F transcription factors and viral oncoproteins, including adenovirus E1A and simian virus 40 (SV40) large T antigen (14, 18, 35, 56). Pocket protein binding to E2F results in active repression of E2F-dependent genes that are required for DNA synthesis and cell cycle progression as well as differentiation and DNA damage checkpoints (3, 53). Overexpression of retinoblastoma family members leads to E2F repression and cell cycle arrest, while phosphorylation of pocket proteins by cyclin-dependent kinases (CDKs) during G_1 and S phases results in dissociation from E2Fs and activation of E2F-dependent gene transcription (22). Interaction of pocket proteins with viral oncoproteins also leads to a loss of E2F binding and repression, providing an important mechanism for virus-mediated transformation (23, 56, 59).

Unique functional roles for each pocket protein are suggested by differential expression during the cell cycle and preferential binding to specific E2Fs. For example, the p130 protein level is elevated in quiescent cells and decreased in proliferating cells, while p107 is absent in quiescent cells and elevated in growing cells (52). While pRb has the strongest affinity for E2F1, E2F2, and E2F3, p130 and p107 preferentially bind to E2F4 and E2F5 (17). Complexes containing p130 and E2F4 and E2F5 are the most abundant pocket protein-E2F complexes in quiescent cells, whereas p107 and E2F4 complexes are predominant in proliferating cells (51). While these observations implicate p130 in the induction or maintenance of the quiescent state in normal cells, the genetic inactivation of all three retinoblastoma family members is required for complete loss of G_1 checkpoint in mouse embryonic fibroblasts (MEFs) (11, 48). In contrast, MEFs prepared from mouse strains with single- or double-knockout members of the retinoblastoma family members were capable of exiting from the cell cycle upon serum deprivation and contact inhibition (8, 29). These results suggested that pocket proteins can substitute for each other in cell cycle control and E2F regulation.

This functional redundancy in cell cycle control does not extend to the developmental regulation by the retinoblastoma family. While the homozygous deletion of the *Rb1* gene results in the embryonic death at mid-gestation, deletion of either p107 or p130 alone does not affect the development and viability of mouse embryos (reviewed in reference 40). Homozygous deletion of both p107 and p130 allowed the full-term development of the embryo but induced abnormalities of the cartilage, bone, and skin, contributing to neonatal lethality (8, 34, 45, 46). This observation suggests that despite overlapping functions in the cell cycle regulation, pRb, p107, and p130 play unique roles in development. Interestingly, deletion of p130 gene in the BALB/c strain resulted in embryonic lethality at midgestation, and a deletion of the p107 gene in this genetic background also caused severe developmental abnormalities that were not observed in mixed-genetic-background mice (31, 32). These differences in the knockout mouse phenotype could be attributed to the reported inactivating allelic variations of CDKN2A, the p16 CDK inhibitor 2A gene, that are found in the BALB/c mouse strain (60, 61).

Unlike pRb and p107, p130 is specifically phosphorylated in growth-arrested and in terminally differentiated cells (4, 22, 38). Notably, the p130 G_0 kinase has not been identified (37). Mass spectroscopy analysis of p130 purified from serum-starved cells revealed a highly phosphorylated region within the B box of the pocket (Fig. 1A) (4, 26, 27). This region spans residues 935 and 1000 of human p130 and is referred to here as the Loop. The Loop region has no sequence homology with the corresponding fragments of p107 and pRb. Earlier reports demonstrate that the Loop region contains a functional nu-

* Corresponding author. Mailing address: Dana-Farber Cancer Institute, Mayer 457, 44 Binney St., Boston, MA 02115. Phone: (617) 632-3825. Fax: (617) 632-4760. E-mail: james_decaprio@dfci.harvard.edu.

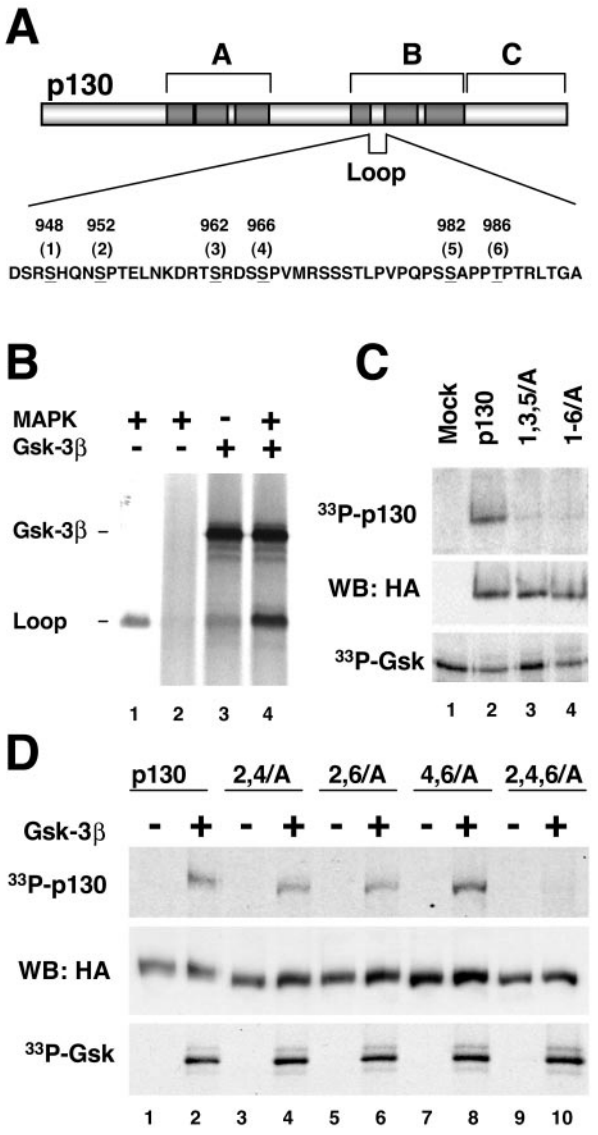

FIG. 1. Unique region of p130 contains three potential GSK3 phosphorylation sites. (A) Schematic structure of p130. The regions forming a pocket domain that is highly conserved among retinoblastoma family proteins are shown darkly shaded. The Loop region in the B-box of p130 is absent in pRb and has no homology with the corresponding region of p107. Residues matching the GSK3 phosphorylation consensus sequence are underlined. Positions of the sites (numbered from 1 to 6 for convenience) correspond to human p130. (B) GSK3 phosphorylates the Loop of p130 in vitro and requires priming phosphorylation. The GST-tagged S935-E1000 fragment (Loop) of p130 was absorbed on glutathione Sepharose beads and subjected to GSK3B (Gsk-3β) phosphorylation in the presence of [γ-^{33}P]ATP either directly (lane 3) or after priming phosphorylation with purified MAPK and nonradioactive ATP followed by extensive washing of the beads (lane 4). A control reaction with MAPK1-prephosphorylated GST-Loop but without GSK3B shows that phosphorylation is mediated by GSK3B and not by residual MAPK1 activity (lane 2). Lane 1 demonstrates phosphorylation of GST-Loop by MAPK1 in the presence of [γ-^{33}P]ATP. An autoradiogram shows phosphorylation of GST-Loop and autophosphorylation of GSK3B. (C) GSK3 phosphorylates p130 but not the 1,3,5/A or 1-6/A p130 mutants. HA-tagged p130 and the mutants were expressed in U-2 OS cells, immunoprecipitated, and incubated with purified GSK3B in the presence of [γ-^{33}P]ATP. An identically prepared sample from vector-transfected cells was used as a control (Mock, lane 1). Reaction products were resolved by SDS-PAGE (10% polyacrylamide gel), transferred to nitrocellulose, and subsequently analyzed by autoradiography and Western blot. The top and bottom panels show the autoradiograms of p130 phosphorylation and GSK3B autophosphorylation, respectively. The middle panel shows a Western blot with anti-HA antibody (WB: HA) confirming that comparable amounts of p130 and the mutants were present in each reaction. (D) GSK3 phosphorylates each of the three pairs of phosphorylation sites in the Loop region of p130. HA-tagged wild-type p130, 2,4/A, 2,6/A, and 4,6/A double mutants and the 2,4,6/A triple mutant were expressed and subjected to GSK3B phosphorylation as described for panel C. For each of the samples, a control reaction without GSK3B indicates that the phosphorylation is mediated by GSK3B and not by other p130-associated kinases (odd lanes). Reaction products were resolved by SDS-PAGE (10% polyacrylamide gel) and transferred to nitrocellulose. The top and bottom panels show the autoradiograms of p130 phosphorylation and GSK3B autophosphorylation, respectively. The middle panel shows a Western blot with anti-HA antibody confirming comparable amounts of p130 and the mutants were present in each reaction.

clear localization sequence and was not required for the growth suppression function of p130 (5, 26). Three pairs of phosphorylated residues in the loop (S948 and S952, S962 and S966, and S982 and T986 in human p130 sequence) matched the consensus pS-X-X-X-pS/pT-P, where X is any residue (Fig. 1A). Importantly, priming phosphorylation of the serine or threonine residue at the 0 position was required for phosphorylation of the corresponding serine residue at the −4 position (26). While the priming phosphorylation of S952 and T986 was most likely mediated by CDK2, phosphorylation of S948, S962, S966, and S982 was CDK independent (26).

Glycogen synthase kinase 3 (GSK3) is a ubiquitously expressed serine-threonine kinase implicated in diverse biological processes, including embryonic development, metabolism, specific gene transcription, and cytoskeleton function (reviewed in references 20, 43, and 57). Notably, GSK3 has been shown to phosphorylate serine or threonine residues at the −4 position after priming phosphorylation of S or T at the 0 position for several substrates in vivo (21, 44, 55). Mammalian GSK3 exists as two isoforms, GSK3A and GSK3B, that share 98% homology in their catalytic domain and have similar biochemical properties. Notably, GSK3 kinase activity is high in resting and nutrient-deprived cells and is negatively regulated upon activation of insulin receptor and Wnt signaling pathways (reviewed in reference 57). Deregulation of these pathways has been implicated in the pathogenesis of human diseases such as type II diabetes and cancer, making GSK3 an important target for biological and pharmacological studies. Here, GSK3 is shown to phosphorylate p130 at specific residues in the Loop region. Our results demonstrate that GSK3 phosphorylation of p130 could be an indication of a unique potentially important function of this retinoblastoma family member.

MATERIALS AND METHODS

Plasmids and recombinant retroviruses. Mutants of p130 were generated by two-step PCR with two overlapping mutagenesis primers (1) using *Pwo* DNA polymerase (Roche Biochemicals). The 5′- and 3′-flanking primers used for all constructs had the following sequences, respectively: F1, 5′CTTCGG GATCTCTGTGCC; and F2, 5′ATAGGGCCCTCTAGATGCATTAAA. Initially, a human p130 cDNA with a silent mutation disrupting an EcoRI site at position 2919 was generated by two-step PCR mutagenesis. This cDNA was then used as a template for PCR to generate p130 phosphorylation site mutants as follows. Fragments of 945 bp with the desired mutations were generated by PCR

with F1 and F2, digested with EcoRI, and inserted into the EcoRI-digested hemagglutinin (HA)-p130/pcDNA 3.1/Zeo expression vector (5). Orientation of inserts was determined by PCR, and mutations were verified by automated DNA sequencing.

To generate retroviral expression vectors, the verified p130/pcDNA3.1 constructs were digested with Bst1107 and ApaI and then inserted into appropriately digested HA-p130/pBabe-Puro vector (provided by H. Land). Recombinant ecotropic retroviruses were produced in Bosc 23 cells transfected with the corresponding pBabe-Puro plasmids (42), harboring p130 inserts as previously described (5, 39).

Cell lines and manipulations. U-2 OS, T98G, and NIH 3T3 cell lines were obtained from American Type Culture Collection and cultured in Dulbecco's modified Eagle's medium supplemented with 10% fetal bovine serum (FBS), 100-U/ml penicillin, and 100-μg/ml streptomycin (Invitrogen). BJ/hTert immortalized human fibroblasts were provided by W. Hahn. To generate U-2 OS-Eco and T98G-Eco cell lines stably expressing murine ecotropic receptor, U-2 OS and T98G cells were transfected with pEcoR/IRES-Neo plasmid (obtained from R. Scully) and selected in G418 (0.4 mg/ml; Gibco).

Cell lines expressing recombinant human p130 and mutants were created by infecting NIH 3T3, U-2 OS-Eco, or T98G-Eco cells with the corresponding recombinant retroviruses followed by antibiotic selection. For induction of G_0/G_1 growth arrest, cells were plated at 50% confluency and incubated in serum-free medium for 72 h. To stimulate entry into the cell cycle, fetal calf serum (20% final concentration) was added to the serum-starved cells. For in vivo inhibition of GSK3, the serum-starved cells were incubated with lithium acetate (47), GSK3 inhibitor II (Calbiochem), SB-216763, or SB-415286 (Biomol). Cell fractionation, flow cytometric analysis of the cell cycle profile, and immunofluorescent cell staining were performed as previously described (5).

Immunoprecipitations and Western blots. Cell extracts for immunoprecipitations and Western blots were prepared in EBC buffer (50 mM Tris-HCl [pH 8.0], 120 mM NaCl, 0.5% Nonidet P-40) supplemented with protease inhibitors (Set I; Calbiochem). The protein concentration of extracts was determined with the D_C protein assay (Bio-Rad). For in vitro phosphatase experiments, 100 μg of cell extract was incubated for 15 min at 30°C with 100 U of λ-phosphatase (NEB) in a buffer provided with the enzyme. For detection of proteins with phospho-specific antibodies and for the cycloheximide chase assay, cell extracts were prepared by lysis in sodium dodecyl sulfate-polyacrylamide gel electrophoresis (SDS-PAGE) loading buffer (60 mM Tris-HCl [pH 6.8], 2% SDS, 10% glycerol) and immediately boiled for 5 min. Typically, 30 μg of whole-cell extract was loaded in the gel for Western blot analysis and 1 mg of the extract was used for immunoprecipitation experiments.

Antibodies. The following antibodies were used for Western blot analysis: rabbit antibodies to p130 (C-20), E2F4 (C-108), p107 (C-18), and cyclin A (H-432) and mouse monoclonal antibody to cyclin E (HE12) (all from Santa Cruz); mouse monoclonal antibody to HA epitope (HA-11) (Covance); rabbit antibodies to phospho-S9-GSK3B (Cell Signaling Technology); and mouse monoclonal antibody to GSK3B (Upstate Biotechnology). Rabbit antibodies to HA epitope (Y-11) from Santa Cruz and mouse monoclonal antibodies to HA epitope (clone 12CA5) and SV40 large T antigen (clone PAb419) were used for immunoprecipitations. The ppRb2 rabbit polyclonal antibodies to diphosphorylated synthetic peptide NH_2-LPVPQPSpSAPPpTPTRLTGA, corresponding to residues 975 to 993 of human p130, were generated and affinity purified by Bethyl Laboratories, Inc.

In vitro phosphorylation assays. A glutathione *S*-transferase (GST)-tagged S935-E1000 fragment of p130 (GST-Loop) was expressed in *Escherichia coli* (DH5α), extracted with B-PER reagent (Pierce), and absorbed on glutathione-Sepharose beads. Washed beads were split into four aliquots and treated as follows. Two aliquots were incubated for 30 min at 30°C with 100 μM ATP, 20 U of p42 mitogen-activated protein kinase 1 (MAPK1; NEB), and 1× MAPK buffer (NEB), and one aliquot was incubated with an identical reaction mixture containing 10 μCi of [γ-^{33}P]ATP (NEN). Beads from two nonradioactive MAPK1 reaction mixtures were then washed three times with 50 mM Tris HCl buffer (pH 7.5) containing 150 mM NaCl and 10 mM EDTA and once with kinase buffer (20 mM Tris HCl buffer [pH 7.5], 10 mM $MgCl_2$, 5 mM dithiothreitol). The remaining aliquot of the beads and one of the nonradioactive MAPK1 reaction mixtures were then incubated for 30 min at 30°C with reaction mixture containing 100 μM ATP, 10 μCi of [γ-^{33}P]ATP, 25 U of GSK3B (NEB), and 1× GSK3 buffer (NEB). The second nonradioactive MAPK1 reaction mixture was incubated with an identical reaction mixture but without GSK3B to control for removal of MAPK1. Reactions were stopped by adding SDS-PAGE loading buffer and analyzed by SDS-PAGE and autoradiography.

For in vitro kinase assays with the full-length p130, cells were extracted with SDS-PAGE loading buffer to disrupt protein complexes and then diluted 10-fold with EBC buffer before immunoprecipitation of p130. Immunoprecipitates were washed three times with EBC and once with kinase buffer (20 mM Tris HCl buffer [pH 7.5], 10 mM $MgCl_2$, 5 mM dithiothreitol) and then incubated for 1 h at 30°C in a reaction mixture containing kinase buffer supplemented with 100 μM ATP and 2 μCi of [γ-^{33}P]ATP per ml in the presence or absence of 25 U of purified GSK3B (NEB).

Cycloheximide chase assay. Exponentially growing U-2 OS cells expressing HA epitope-tagged p130 or the indicated phosphorylation site mutants were plated onto six-well plates 24 h before the experiment. The cells were incubated with 30 μg of cycloheximide per ml and 25 μM MG132, as indicated in Fig. 5B. At indicated time points, the cells were rinsed with phosphate-buffered saline and extracted with SDS-PAGE loading buffer. An equal amount of protein extracts was loaded in the gel, and the expression of p130 and mutants was analyzed by SDS-PAGE followed by Western blot with anti-HA antibody. The intensity of the protein bands on the Western blot was quantified with Fluor-S MultiImager and Quantity One software (Bio-Rad). The same membranes were reprobed with antivinculin antibody, and the quantified intensity of vinculin bands was used to normalize the results of the HA Western blots.

RESULTS

GSK3 specifically phosphorylates residues in the Loop region of p130. The Loop region within the B-pocket domain of p130 contains three pairs of phosphorylated residues matching the consensus pS-X-X-X-pS/pT-P (Fig. 1A) (4). Phosphorylation of two sites (S948 and S982) was shown to be dependent on the priming phosphorylation of S952 and T986 at position +4, respectively (26). GSK3, a ubiquitous serine/threonine protein kinase, preferentially phosphorylates a serine or threonine residue in a position −4 relative to a prephosphorylated S or T residue (21). To test whether GSK3 could phosphorylate the loop of p130 and required a priming phosphorylation, a GST-tagged S935-E1000 fragment of p130 was incubated with recombinant GSK3B and radioactive ATP directly or after prephosphorylation by a proline-directed protein kinase, MAPK1 (13). As shown in Fig. 1B, although GSK3B directly phosphorylated purified GST-Loop fusion protein weakly, this phosphorylation was dramatically facilitated by MAPK1 prephosphorylation.

To test whether GSK3 will specifically phosphorylate full-length p130 protein, wild-type p130 or two mutants carrying alanine substitutions for the potential GSK phosphorylation and priming sites (mutants with sites 1, 3, and 5 changed to A [1,3,5/A] and sites 1 to 6 changed to A [1-6/A]; Fig. 1A) were subjected to GSK3 phosphorylation in vitro. For this experiment, HA-tagged p130 and mutants were transiently expressed in U-2 OS cells, immunoprecipitated with anti-HA antibodies, and incubated in the presence of radioactive γ-ATP and purified GSK3B. As shown in Fig. 1C, wild-type p130 was phosphorylated under these conditions (^{33}P-p130), while either mutant was not. Western blot with anti-HA antibodies revealed equal amount of p130 species in the reactions (Fig. 1C, WB: HA). The GSK3 autophosphorylation was also comparable in all samples (^{33}P-GSK). Therefore, mutation of either putative GSK3 sites (S948, S962, and S982) or priming phosphorylation sites (S952, S966, and T982) abolished phosphorylation of p130 by GSK3 in the context of full-length protein.

To test whether each of the three S-X-X-X-S/T-P sites in the loop of p130 could be phosphorylated by GSK3B, three double mutants where two of three priming phosphorylation sites (S/T-P) were substituted for with alanine (2,4/A, 2,6/A, and 4,6/A), as well as a triple mutant in which all three priming sites were mutated (2,4,6/A), were prepared (Fig. 1). We subjected

these mutants to an in vitro GSK3B phosphorylation as described in the previous experiment and found that while the triple mutant (2,4,6/A) was not phosphorylated under these conditions, the wild-type p130 and each of the double mutants were readily phosphorylated by GSK3B (Fig. 1D). Taken together, these results demonstrate that p130 can serve as a substrate for GSK3 in vitro and that the phosphorylation of p130 by GSK3 at the S948, S962, or S982 sites is dependent on priming phosphorylation at S952, S966, and T986 residues within the Loop.

Inhibition of GSK3 in vivo dramatically affects G_0/G_1 phosphorylation forms of p130. GSK3 kinase activity is present in growth factor-deprived cells (28, 57) when p130 is specifically phosphorylated (4, 22, 38). We tested whether inhibition of GSK3 under the serum-starved conditions would affect phosphorylation of p130. T98G cells were serum starved for 72 h and then treated with 25 mM lithium acetate (47) or 25 μM small-molecule GSK3 inhibitor II (41) for 3 h prior to extraction. For comparison of the p130 phosphorylation status in the control and drug-treated samples, an aliquot of each sample was treated with λ-phosphatase before Western blot analysis. A sample prepared from the cells grown in the presence of 10% serum was used to show the gel migration of hyperphosphorylated form 3 of p130 (Fig. 2A, lanes 1 and 3 or 6). As shown in Fig. 2A, treatment with lithium or inhibitor II led to a marked reduction in gel migration of p130 in serum-starved T98G cells (compare lanes 3 and 4 or 6 and 7). Treatment of the samples with λ-phosphatase resulted in a complete loss of p130 phosphorylation and produced p130 form 1a that migrated identically in untreated and drug-treated series (Fig. 2A, lanes 2, 5, and 8). These results suggest that the difference in gel migration of p130 before and after GSK3 inhibition was phosphorylation related. From this experiment, we conclude that inhibition of GSK3 in serum-starved T98G cells results in a specific loss of G_0/G_1-specific phospho forms of p130.

Next, we tested whether endogenous p130 isolated from serum-starved cells could be phosphorylated by GSK3 in vitro and whether this phosphorylation could be enhanced by pretreatment with a GSK3 inhibitor. T98G cells were serum deprived for 72 h and then treated with 25 mM lithium acetate for 3 h prior to extraction and immunoprecipitation of endogenous p130. Immunoprecipitates were incubated in the presence of radioactive γ-ATP and recombinant GSK3B and analyzed by SDS-PAGE followed by autoradiography and Western blot. As shown in Fig. 2B, the endogenous p130 isolated from G_0/G_1-arrested T98G cells could be specifically phosphorylated by GSK3B. Lithium treatment of the cells enhanced GSK3-dependent phosphorylation 2.5-fold (Fig. 2B, compare lanes 4 and 8 on the ^{33}P-p130 panel). Together with a decrease of p130 G_0/G_1 phosphorylation upon lithium treatment (described above), this result is consistent with specific p130 residues dephosphorylated upon inhibition of GSK3 in vivo that can be rephosphorylated by GSK3B in vitro.

In vivo inhibition of GSK3 by serum stimulation induces a transient loss of the G_0 phosphorylation forms of p130. GSK3 basal activity is high in growth factor-deprived cells and is reduced upon treatment with growth factors through an inhibitory phosphorylation on the serine 21 or serine 9 residue in GSK3A or GSK3B, respectively (10, 21). Given that p130 is phosphorylated in serum-starved cells, we determined whether inhibition of GSK3 upon addition of growth factors would affect p130 phosphorylation. For this experiment, we chose nontransformed human BJ/hTERT fibroblasts (25) immortalized by introduction of human telomerase for their high growth factor dependency and for the absence of the mutations in the components of the growth factor receptor pathways that are often found in cancer cells. BJ/hTERT cells were serum starved for 48 h and then treated with 20% serum and analyzed for the phosphorylation status of endogenous p130 and GSK3B (Fig. 2C and D). Cell cycle progression induced by serum restimulation was monitored by fluorescence-activated cell sorter analysis of DNA (Fig. 2D). Western blot for p130 revealed the presence of phospho form 2 in serum-starved cells (0 h). Starting from 2 h after serum addition, phospho form 2 of p130 became less prominent until it reappeared at 8 h after serum stimulation (Fig. 2C, WB: p130). S9-phosphorylated (pS9, inactive) GSK3B signal was increased immediately after serum addition and then started to decline after 8 h and reached the basal level by 19 to 21 h, while the levels of total GSK3B remained unchanged throughout the experiment (Fig. 2C). Therefore, inhibition of GSK3 induced by serum stimulation of BJ/hTERT cells precedes and coincides with a decrease in the G_0-specific phosphorylation of p130. Interestingly, GSK3B appears to be reactivated as early as at 8 h after serum addition and therefore could potentially contribute to the hyperphosphorylation of p130 during the G_1/S-phase transition (Fig. 2C, WB: p130, form 3).

The decrease in p130 phosphorylation in BJ/hTERT cells after serum addition correlated temporally with the loss of GSK3 activity. To test whether this effect could be detected in other cell types, we serum-starved T98G human glioblastoma cells and mouse NIH 3T3 cell line engineered to express HA-tagged human p130 for 48 h and then treated them either with 20% serum or with 20 mM lithium acetate. As shown in Fig. 2E, the G_0/G_1-specific phospho forms (1 and 2) of both endogenous and HA-tagged p130 were reduced within 3 h of serum or lithium treatment. Further incubation with serum (8 h) resulted in the appearance of hyperphosphorylated p130 species (form 3), while continued lithium treatment led to a sustained decrease in p130 phosphorylation that remained unchanged for up to 24 h (data not shown). Additionally, at the 8-h time point in lithium-treated series, we observed a significant decrease in the p130 protein levels (compare lanes 1 and 2 on Fig. 2E). Taken together, the results presented above strongly indicate that GSK3 contributes to the in vivo phosphorylation of p130 in different cell types.

Phosphorylation of p130 by GSK3 detected by phospho-specific antibodies. To further confirm that GSK3 phosphorylates p130 in vivo, rabbit antibodies were generated against a synthetic peptide containing phosphorylated residues S982 and T986 of human p130 (Fig. 1A). These affinity-purified antibodies (designated ppRb2) could detect endogenous p130 in whole-cell extracts prepared from serum-starved T98G cells and displayed high specificity toward diphosphorylated form of p130. As shown in Fig. 3A, ppRb2 antibodies recognize a protein band comigrating with p130 as detected by the C-terminus-specific antibodies (C-20). In a peptide competition assay, the diphosphorylated pS982/pT986 peptide was able to efficiently block this cross-reactivity (Fig. 3A, lanes 7 to 9), while the nonphosphorylated form of the same peptide was

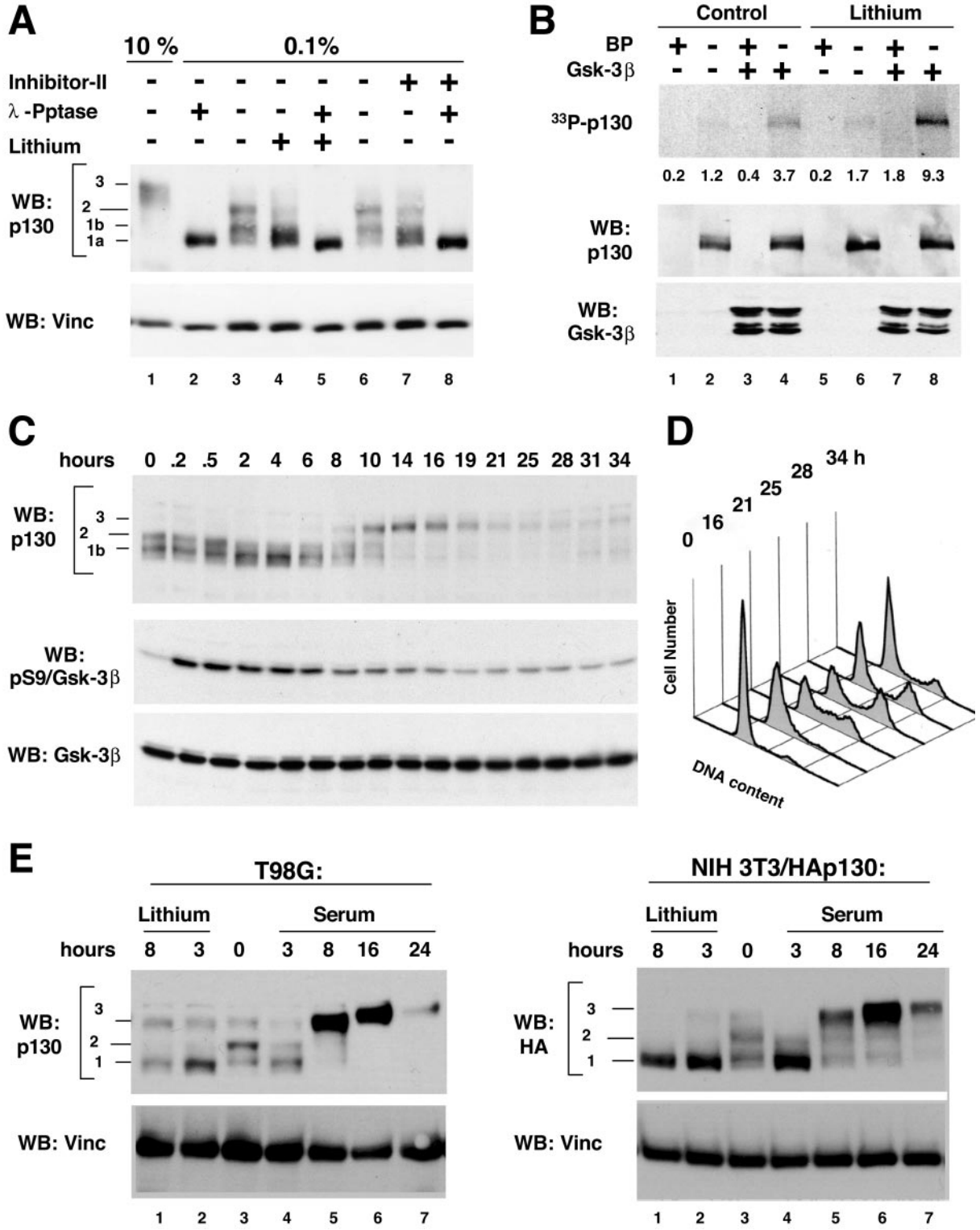

FIG. 2. Inhibition of GSK3 in G_0/G_1-arrested cells leads to a disappearance of specific phospho forms of p130. (A) Inhibition of GSK3 in serum-starved cells results in dephosphorylation of the endogenous p130 in T98G glioblastoma cells. Panel A shows a Western blot (WB) of p130 in extracts prepared from T98G cells that were arrested in G_0 by serum deprivation (lanes 2 to 8) and left untreated (lanes 2 and 3) or treated for 3 h with 25 mM lithium acetate (lanes 4 and 5) or 25 μM GSK3 inhibitor II (lanes 7 and 8). Cell extracts were resolved by SDS-PAGE (6% polyacrylamide gel) prior to blotting onto the nitrocellulose paper. To compare the migration of GSK3 inhibitor-treated and dephosphorylated p130, samples in lanes 2, 5, and 8 were treated with λ-phosphatase (λ-Pptase) prior to loading. A sample prepared from cycling T98G cells (10% FBS, lane 1) is shown to emphasize the difference in gel migration of specific phospho forms of p130 (forms 1a, 1b, 2, and 3, shown to the side). (B) Enhanced GSK3 phosphorylation of p130 from lithium-treated cells compared to intact cells. T98G cells were arrested in G_0 by serum deprivation and left untreated (lanes 1 to 4) or treated for 3 h with 25 mM lithium acetate (lanes 5 to 8) prior to lysis and immunoprecipitation

unable to compete even at a 10-fold-higher concentration (Fig. 3A, lanes 3 to 5). To further test the specificity of the phospho-specific antibodies, a Western blot was performed against the 1,3,5/A and 2,4,6/A mutants of p130. The wild-type p130 and the mutants were expressed in G_0/G_1-arrested NIH 3T3 cells, immunoprecipitated with anti-HA antibody, and Western blotted with ppRb2. Figure 3B (WB: ppRb2) shows that only the wild-type p130, but neither of the mutants, was detected by ppRb2, although all proteins were present in the immunoprecipitates (WB: HA). These experiments strongly suggest that ppRb2 antibody predominantly cross-reacts with p130 that is phosphorylated at serine 982 and threonine 986.

Next, ppRb2 antibodies were used to detect p130 phosphorylation changes upon inhibition of GSK3 in vivo. T98G cells were serum starved for 72 h and then treated for 3 h with the GSK3 inhibitory compounds, lithium acetate and small-molecule inhibitors GSK3 inhibitor II (41), SB-216763, and SB-415286 (9). Unphosphorylated p130 was prepared from an aliquot of T98G extract incubated with λ-phosphatase and served as a control. As shown in Fig. 3C, treatment of the cells with GSK3 inhibitors resulted in a dramatic reduction of ppRb2 recognition of p130 in the cell extracts, similar to that induced by λ-phosphatase treatment of the sample. The total amount of p130 in the extracts was unaffected by the treatments (Fig. 3C, WB: C-20), although the doublet present in the G_0 extracts collapsed to the faster-migrating form 1. This result shows that the loss of ppRb2 recognition could be attributed to a loss of phosphorylation at S982, T986, or both of these sites in p130. Since phosphorylation of T986 site in p130 was previously shown to be CDK dependent and since lithium, SB-216763, and SB-415286 are known not to inhibit other kinases at the concentrations used in this experiment (9, 12), it is most likely that inhibition of GSK3 here induced dephosphorylation of p130 at position S982. However, whether this event could also trigger dephosphorylation of the T986 site via an indirect mechanism remains to be established.

Phosphorylation of the p130 Loop mutants. To determine if the p130 mutants with altered GSK3 and priming phosphorylation sites in the Loop were affected by cell cycle-dependent phosphorylation, we generated stable cell lines expressing HA epitope-tagged wild-type p130 and the mutants of interest. We have previously characterized a p130 deletion mutant lacking the entire Loop region (ΔLoop, with deletion of residues 935 to 997) (4). In addition, we generated several mutants in which specific phosphorylation sites in the Loop were replaced either with alanine to prevent phosphorylation or with aspartic acid residues to mimic a negative charge created by phosphorylation. Using retrovirus-mediated gene transfer followed by antibiotic selection to obtain polyclonal cell populations stably expressing recombinant forms of p130, we generated such cell lines in NIH 3T3 mouse fibroblasts and the T98G human glioblastoma cell background. Ectopic expression of recombinant p130 and mutants resulted in a moderate increase of the total p130 levels that did not affect growth rates of the resulting cell lines (data not shown).

The gel migration patterns of the p130 and phosphorylation site mutants, in which phosphorylation sites in the Loop were substituted for with alanine (1-6/A) or aspartic acid residues (1-6/D), were compared in the NIH 3T3 cells grown in the presence of high (10%) and low (0.1%) percentages of serum. In addition, the serum-starved cell lines were treated with 20 mM lithium acetate for 3 h to test the effect of GSK3 inhibition on the phosphorylation of p130 and mutants. As shown in Fig. 4A, both alanine and aspartic acid substitution in the Loop sites resulted in altered gel migration of p130 both in the presence and in the absence of serum (compare lanes 1, 4, and 7 and lanes 2, 5, and 8). While the wild-type p130 was present as a set of G_0/G_1 forms 1 and 2 that were sensitive to lithium, both 1-6/A and 1-6/D mutants migrated as single bands unaffected by the lithium treatment (lanes 2 and 3, 5 and 6, and 8 and 9). Next, we compared phosphatase sensitivity of the wild-type p130 and mutants expressed in NIH 3T3 cells grown under high- and low-serum conditions. Figure 4B shows an anti-HA Western blot of λ-phosphatase-treated extracts prepared from cells expressing the wild-type p130, 1-6/A, or 1-6/D mutants. Both mutants, as well as the wild-type p130, displayed significant phosphatase sensitivity when expressed under high-serum conditions (lanes 1 to 6), while only the wild-type p130, but not mutants, could be dephosphorylated when extracted from the serum-starved cells (lanes 7 to 12). Insensitivity of the 1-6/A and 1-6/D mutants to the lithium or phosphatase treatment under serum-starved conditions further supports the conclusion that phosphorylation of p130 in G_0/G_1 is specific to the Loop region and is mediated by GSK3. In addition, our data indicate that phosphorylation of the Loop sites contributes to gel migration pattern of form 3 of p130 in proliferating cells (compare lanes 1, 3, and 5, Fig. 4A).

with anti-p130 C-20 antibodies. Control samples were immunoprecipitated in the presence of the C-20 blocking peptide (BP) to ensure the specificity of the reactions (odd lanes). Samples were resolved by SDS-PAGE (7.5% polyacrylamide gel) and transferred to nitrocellulose. The upper panel shows an autoradiogram of p130 (^{33}P-p130) and the PhosphorImager quantification of the p130 signal. Western blot panels of p130 and GSK3B show that equal amounts of these proteins were present in each reaction. (C) Serum restimulation of BJ/hTert fibroblasts results in transient dephosphorylation of p130, coinciding with inactivation of GSK3. BJ/hTert cells were synchronized in G_0 and then treated with 20% serum for the indicated time. Cell extracts were resolved by SDS-PAGE (6% polyacrylamide gel for p130 and 10% polyacrylamide gel for GSK3 analysis, respectively) prior to blotting onto nitrocellulose paper. Western blots show the changes in phosphorylation of p130 occurring during the exit of the cells from the G_0-arrested state and the kinetics of GSK3 inactivation, monitored by phosphorylation of the serine 9 residue (pS9) of GSK3B. The membrane was stripped and reprobed with anti-GSK3B antibodies to ensure equal loading of the samples (Gsk-3β). (D) FACS analysis of DNA content of BJ/hTert cells from the experiment shown on panel C. (E) Serum restimulation results in a transient decrease of G_0/G_1 phosphorylation of p130 in T98G cells, while treatment with lithium leads to a sustained loss of G_0/G_1 phosphorylation. The left panels show a Western blot of p130 in T98G cells that were serum starved for 72 h to induce the G_0/G_1 state (lane 3) and treated with 25 mM lithium acetate (lanes 1 and 2) or 20% fetal calf serum (lanes 4 to 7) for the indicated time. The right panels show a Western blot of the HA-tagged recombinant human p130 stably expressed in NIH 3T3 cells that were serum starved and treated as described above. Cell extracts were resolved by SDS-PAGE (6% polyacrylamide gels) prior to blotting. Membranes were reprobed with antivinculin antibodies to demonstrate equal loading of the samples (WB: Vinc).

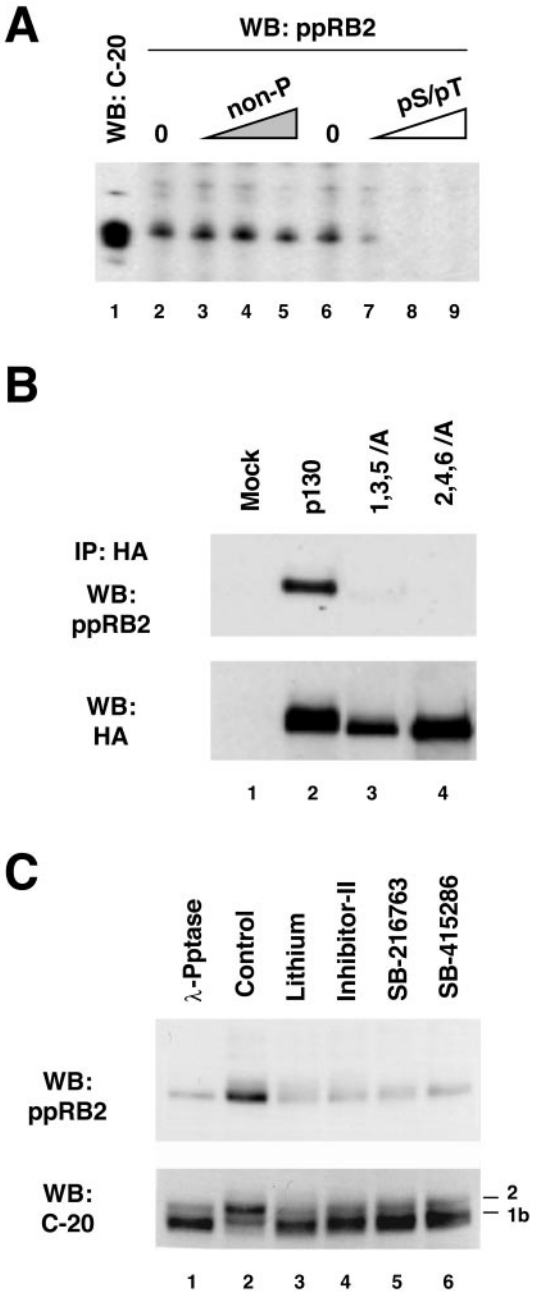

FIG. 3. In vivo phosphorylation of p130 detected by phospho-specific antibodies to GSK3 sites in p130. (A) Characterization of the phospho-specific antibodies raised against pS982/pT986. Whole-cell extract prepared from G_0-arrested T98G cells was run in a preparative single-well gel (7.5% acrylamide), transferred to nitrocellulose, and incubated with the C-20 anti-p130 antibody (lane 1) or ppRb2 phospho-specific anti-p130 antibodies (both at 200 ng/ml) in a multi-slot screening cassette. Phospho-specific antibodies were used directly (lanes 2 and 6) or after preincubation with the indicated blocking peptides. Blocking peptides were used at following concentrations: nonphosphorylated peptide (non-P) at 20, 200, and 2,000 ng/ml and the double-phosphorylated phosphopeptide (pS/pT) at 2, 20, and 200 ng/ml. WB, Western blot. (B) Phospho-specific ppRb2 antibodies do not cross-react with p130 mutants with inactivated GSK3 phosphorylation sites. The top panel shows HA-tagged p130, 1,3,5/A, and 2,4,6/A mutants stably expressed in NIH 3T3 cells, immunoprecipitated (IP) with anti-HA antibodies, resolved by SDS-PAGE (6% polyacrylamide gel), and blotted with ppRb2 antibodies. Parental NIH 3T3 cells were used as a control (lane 1). The cells were arrested by serum deprivation for 48 h prior to the experiment. The blot was reprobed with anti-HA antibody to show comparable amount of proteins in the immunoprecipitates (bottom panel). (C) Inhibition of GSK3 in G_0-arrested cells leads to a decreased recognition of p130 by ppRb2. T98G cells were arrested in G_0 by serum deprivation and left untreated (lanes 1 and 2) or treated with lithium acetate (25 mM, lane 3), GSK3 inhibitor II (25 μM, lane 4), SB-216763 (30 μM, lane 5), or SB-415286 (100 μM, lane 6) for 3 h. Untreated extracts in lane 1 were incubated with λ-phosphatase (λ-Pptase) before loading. The upper panel shows the ppRb2 Western blot of whole-cell extracts resolved by SDS-PAGE (6% polyacrylamide gel). The bottom panel shows the same membrane after stripping and reprobing with C-20 anti-p130 antibody.

Cell cycle-dependent regulation of the p130 Loop mutants. Cell cycle-dependent regulation of p130 includes CDK-mediated phosphorylation and proteosomal degradation in the S phase (26, 37, 54). We observed that HA-tagged p130 stably expressed in NIH 3T3 cells also undergoes cell cycle-dependent phosphorylation and specific changes in its expression levels (Fig. 2E, WB: HA). Similarly to the changes observed for endogenous p130, HA-p130 in NIH 3T3 cells was present as phospho forms 1 and 2 in G_0-arrested cells and as hyperphosphorylated (form 3) at 8 h after serum stimulation and displayed significantly decreased overall expression levels at 24 h (Fig. 2E, WB: p130). To determine whether the Loop contributes to the cell cycle-dependent stability of p130, NIH 3T3 cells expressing p130, 1-6/A or 1-6/D mutants were synchronized in G_0/G_1 and then in early S phase and released to continue the cell cycle and used for Western blot analysis with anti-HA antibody (Fig. 5A). A Western blot for cyclin B1 shown in Fig. 5A serves as a marker of the cell cycle progression, since it is absent in G_0/G_1, expressed in S phase, and degraded upon exit from mitosis. As seen in Fig. 5A, both of the Loop mutants as well as the wild-type p130 underwent phosphorylation in S phase (lanes 2, 8, and 14). Upon completion of the cell cycle (evident from disappearance of cyclin B1), hypo- or unphosphorylated species of p130 and mutants accumulated in all three series (lanes 6, 12, and 18). A decrease in the protein levels upon progression through the S and G_2 phases was also similar in all three series (lanes 4 and 5, 10 and 11, and 16 and 17), although the 1-6/A mutant S/G_2 expression levels were slightly lower than those of the wild type and 1-6/D mutant. This experiment demonstrates that the Loop of p130 is not involved in the cell cycle-dependent regulation of p130, including the changes of the expression levels, hypophosphorylation in G_0 and G_1 and hyperphosphorylation in S phase.

Alanine substitution in the Loop phosphorylation sites in p130 results in a decreased stability of the protein. The expression level of the 1-6/A mutant observed in the cells progressing through the cell cycle was lower than those in the wild-type or 1-6/D p130 (Fig. 5A). We determined whether this mutant had a shorter half-life than the wild-type p130. U-2 OS cells have been previously used to demonstrate the proteosome-mediated degradation of p130 and to determine the half-life of ectopically expressed p130 (54). We generated polyclonal U-2 OS cell lines stably expressing wild-type p130 as well as 1,3,5/A, 1-6/A, or 1-6/D mutants. The cell lines expressed similar levels of the recombinant p130 species, and their growth rates were unaffected by recombinant protein expres-

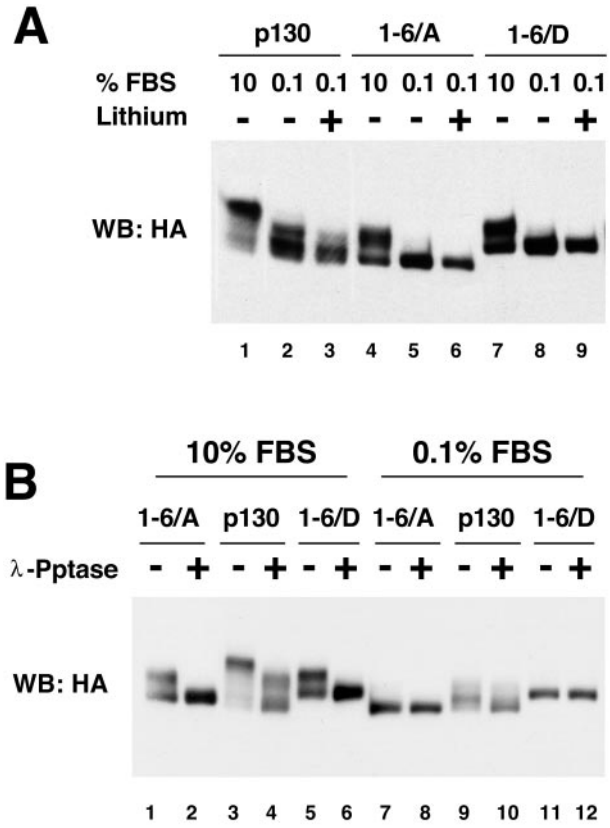

FIG. 4. Characterization of the Loop phosphorylation site mutants of p130. (A) Substitution mutations of the Loop phosphorylation sites in p130 result in an altered gel migration and a loss of lithium sensitivity. NIH 3T3 cells stably expressing HA-tagged p130, 1-6/A, and 1-6/D mutants were grown in standard medium (10% FBS, lanes 1, 4 and 7), serum-starved for 48 h prior to lysis (0.1% FBS, lanes 2, 5, and 8), or serum starved and treated with 25 mM lithium acetate for 3 h prior to lysis (lanes 3, 6, and 9). Lysates were resolved by SDS-PAGE (6% polyacrylamide gel). A Western blot (WB) with anti-HA antibody shows changes in gel migration of p130 and mutants upon treatment. (B) Mutations of the phosphorylation sites in the Loop of p130 result in a loss of phosphatase sensitivity in G_0-arrested but not in cycling cells. A Western blot of HA-tagged p130 and 1-6/A and 1-6/D mutants stably expressed in NIH 3T3 cells and resolved by SDS-PAGE (6% polyacrylamide gel) is shown. The cells were grown in the standard medium (10% FBS, lanes 1 to 6) or arrested by serum deprivation for 48 h prior to lysis (0.1% FBS, lanes 7 to 12). The extracts were incubated with or without λ-phosphatase (λ-Pptase) (odd or even lanes, respectively) prior to loading.

sion (data not shown). Figure 5B (WB: HA) shows a representative Western blot of p130 and the mutants expressed in U-2 OS cells treated with cycloheximide for different times (lanes 1 to 4) or treated for 4 h with cycloheximide and proteosome inhibitor MG132 (33) (lane 5). A graphic representation of the quantitative analysis of p130 and the mutant expression levels determined in at least three independent cycloheximide chase experiments is shown in Fig. 5B, bottom panel. These data demonstrate that the wild-type p130 and 1-6/D mutant displayed similar half-lives significantly exceeding 4 h, while both of the mutants with alanine substitution (1,3,5/A and 1-6/A) had shorter half-lives of approximately 4 h. The proteosome inhibitor MG132, when added together with the cycloheximide, was able to block the degradation of the wild-type p130 as well as the mutants regardless of the status of the Loop. Therefore, phosphorylation of the Loop contributes to stability of p130 without affecting its proteosomal degradation.

DISCUSSION

The cell cycle-dependent phosphorylation of RBL2/p130 has been extensively studied. Recently, 22 serine and threonine residues in p130 were identified that were phosphorylated in vivo (4, 26, 27). Furthermore, it was suggested that three types of kinases, including cyclin D-CDK4/6, cyclin A/E-CDK2, and non-CDK kinase(s), converge to phosphorylate p130 on these residues. Intriguingly, all identified non-CDK phosphorylation sites in p130, including S948, S966, S962, and S982, were clustered in a short nonconserved region within the B-domain (26). Here, we demonstrate that three of these residues, namely S948, S962, and S982, are phosphorylated in vivo by the non-CDK kinase, GSK3. The Loop region of p130, as well as the phosphorylation sites present in the Loop, is not conserved in other pocket proteins, suggesting a unique regulatory role for these phosphorylation sites in p130.

The previous study demonstrated that the non-CDK-dependent phosphorylation at residues S948 and S982 in p130 required priming phosphorylation at CDK-dependent sites (26). Our data here show that GSK3 phosphorylation of p130 Loop can be enhanced by priming phosphorylation by a proline-directed kinase (MAPK1) in vitro (Fig. 1B). Moreover, the finding that GSK3 phosphorylation of full-length p130 was equally efficiently blocked by either the combined mutation of the S948, S962, and S982 phosphorylation sites in the Loop or S952, S966, and T986 sites (Fig. 1C) strongly supports a priming phosphorylation-dependent mechanism of GSK3 phosphorylation of p130. Priming-dependent phosphorylation is characteristic for many known substrates of GSK3, including the classical substrate glycogen synthase (10, 21, 55, 57). Such a mechanism creates a basis for an involvement of GSK3 in regulation of a diverse variety of cellular proteins and provides specificity of the regulation of GSK3 substrates by integrating multiple signaling pathways. It remains unclear whether CDKs could mediate the priming phosphorylation of the p130 Loop sites in the context of the G_0/G_1-arrested cells where CDK activity is dramatically down-regulated or whether other proline-directed kinases could be responsible for this phosphorylation. Since a significant part if not all of the p130 protein pool undergoes proteosomal degradation in S phase of the cell cycle (54), the second possibility appears more likely. Another intriguing question that remained outside the scope of this study is whether GSK3 that appears only transiently inactivated upon serum restimulation of the serum-starved G_0/G_1-arrested cells (Fig. 2C) could contribute to the hyperphosphorylation of p130 in late G_1/S phase.

To study the functional role of the p130 Loop phosphorylation, we created stable cell lines ectopically expressing moderate levels of recombinant p130 proteins. Initial characterization of the p130-expressing cell lines revealed that the recombinant p130 undergoes cell cycle-dependent regulation similar to the endogenous p130 protein, including the changes in phosphorylation and expression levels. Therefore, this ex-

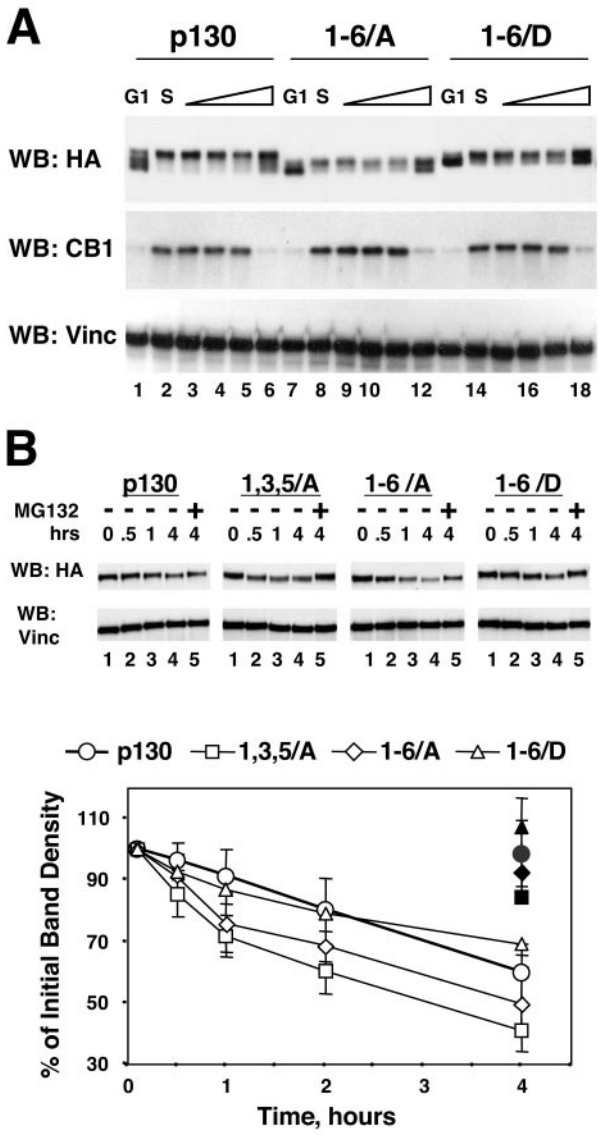

FIG. 5. Cell cycle-dependent expression of the Loop phosphorylation site mutants of p130. (A) Phosphorylation site mutants of the Loop of p130 expressed in NIH 3T3 cells undergo cell cycle-dependent changes. NIH 3T3 cells stably expressing HA-tagged p130, 1-6/A, or 1-6/D mutants were arrested in G_0/G_1 by serum deprivation (lanes 1, 7, and 13) and further synchronized in early S phase by incubation for 16 h with medium supplemented with 20% FBS and 1 mM hydroxyurea (lanes 2, 8, and 14). The medium was then replaced with standard growth medium (10% FBS), and the cells were allowed to continue the cell cycle for an additional 2, 4, 6, or 10 h (lanes 3 to 6, 9 to 12, and 15 to 18). The upper panel shows a Western blot (WB) of p130 and mutants detected with anti-HA antibody, the middle panel is a Western blot of cyclin B1, and the bottom panel shows the same membrane stripped and reprobed with antivinculin (Vinc) antibody to confirm equal loading of the samples. (B) Alanine substitution in the Loop phosphorylation sites in p130 results in a decreased stability of mutant proteins. U-2 OS cells stably expressing HA-tagged p130 and the indicated mutants were incubated for 0, 0.5, 1, and 4 h with cycloheximide (lanes 1 to 4) or for 4 h with cycloheximide and proteosome inhibitor MG132 (33) (lane 5). Expression of p130 and the mutants was analyzed by SDS-PAGE (10% polyacrylamide gels) followed by Western blot with anti-HA antibody and quantitatively evaluated by densitometry. Representative Western blots are shown in the top panel. The same membrane was stripped and reprobed with antivinculin antibody to ensure equal loading of the samples. The amount of p130 was normalized by vinculin and expressed as a percentage of the value taken at time zero. Filled symbols on the graph show the values of the corresponding MG132-treated series. The graph shows average values and standard deviation of at least three experiments.

perimental system allowed us to study the regulation of mutant p130 proteins in the context of the cell cycle and to analyze their functional interactions while avoiding overexpression conditions that could result in artifacts. Using NIH 3T3 cells stably expressing phosphorylation site mutants of p130, we found that the alanine or aspartic acid substitution of the phosphorylated residues in the Loop (1-6/A or 1-6/D, Fig. 1A) (4) results in a complete loss of the G_0/G_1-specific phosphorylation of the mutant p130 proteins (Fig. 4). These mutants, however, were able to undergo CDK-dependent phosphorylation both in asynchronous cells and in synchronized cells upon the G_1/S transition (Fig. 4 and 5A). This result is in agreement with the previously reported p130 mutagenesis data where the alanine substitution in 12 phosphorylation sites (including 6 residues in the Loop region) did not affect the phosphorylation of the remaining 9 sites (19).

We also used the p130 stable cell lines to test whether the Loop phosphorylation is essential for interactions of p130 with its known cellular partners. Alanine substitution in some or all phosphorylation sites in the Loop region of p130 does not affect its ability to interact with E2F4 in transient transfection experiments (4, 19, 26). However, given that the Loop sites in p130 were clearly phosphorylated in G_0/G_1-arrested cells where p130 is predominantly associated with E2F4, we tested the possibility of whether the mutation mimicking the "constantly phosphorylated" state of the Loop will result in more efficient or sustained binding of p130 with E2F4. Using stable cell lines expressing 1-6/A or 1-6/D mutants of p130 to monitor their interaction with E2F4 in the context of the cell cycle, we did not observe any differences in the efficiency or the dynamics of this binding (unpublished data). Unlike pRb, which exhibits its growth suppression activity mainly through the repression of E2Fs, both p107 and p130 are able to block the cell cycle progression by binding cyclin A- or E-CDK2 complexes that has been shown to inhibit the activity of these kinase complexes (reviewed in references 6 and 24). While the p130 mutagenesis study published previously found the binding of cyclin A or E with p130 to be phosphorylation independent (26), another report suggested that cyclins A and E could preferentially bind to specific phosphorylated forms of p130 in the endogenous immunoprecipitation experiments (30). We found that both 1-6/A and 1-6/D mutants were able to bind cyclins similarly to the wild-type p130 (unpublished data). In addition, we were able to detect both E2F4 and cyclin E in the cell-cycle-specific complexes with endogenous p130 immunoprecipitated with the phospho-specific ppRb2 antibodies (unpublished data). Our results therefore demonstrate that interaction of p130 with E2F4 and G_1/S cyclins is not affected by phosphorylation status of the Loop.

Transformation of certain cell types by SV40 large T antigen is mediated in part by interaction of T antigen with retinoblastoma family proteins, including p107 and p130 (59). This interaction has been shown to be dependent on the integrity of the LXCXE motif in T antigen and a subset of conserved

amino acid residues in the B-domain of pocket proteins (Y709 and K713 in pRb and Y879 and K901 in p130) (5, 15, 59). We hypothesized that close proximity of the highly phosphorylated Loop region could influence the interaction between T antigen and p130. However, both 1-6/A and 1-6/D mutants of p130 as well as the ΔLoop mutant were able to bind to T antigen, demonstrating that an intact Loop is not required for this interaction (unpublished data).

The Loop region of p130 contains a functional nuclear localization signal, ^{935}KRKRR^{939} (5), located in the vicinity of the GSK3 phosphorylation sites. Phosphorylation of cyclin D1 by GSK3 promotes its nuclear export (16). We looked into cellular localization of p130 mutants where phosphorylation sites in the Loop were replaced with alanine (1,3,5/A and 1-6/A) or aspartic acid residues (1-6/D) and could not detect any differences in nuclear localization of these p130 mutants (unpublished data). Additionally, we have previously found that p130 accumulates in the cytoplasm upon G_1/S transition due to the nuclear export (5). Given the possibility that GSK3 could be reactivated in S phase, we tested whether 1-6/A mutations or 1-6/D mutations in the Loop would affect nuclear export of p130. We found that the nucleocytoplasmic distribution of the p130 Loop mutants was very similar to that of the wild-type p130 in synchronized cells (unpublished data), indicating that both nuclear localization of p130 and its nuclear export in S phase were independent of the phosphorylation status of the Loop.

In summary, the results discussed above demonstrate that the Loop region in the B pocket of p130 harbors residues that are responsible for G_0/G_1 phosphorylation of p130. This region, however, is not essential for the known functions of p130 associated with its ability to block the cell cycle progression, including interaction with E2F4, cyclins A and E, and the LXCXE-containing proteins. However, we found that the stability of p130 mutants where the Loop could not be phosphorylated (1,3,5/A and 1-6/A) was modestly reduced compared to that of the wild-type p130 (Fig. 5B and C). p130 has been shown to be targeted to proteosomal degradation by SCF^{SKP2} ubiquitin-ligase complex, and this degradation is thought to be triggered by phosphorylation of p130 by CDK4/6 at S972 in the spacer domain (2, 54). Our results show that the degradation of the wild-type p130, as well as the Loop phosphorylation site mutants 1,3,5/A, 1-6/A, and 1-6/D, was inhibited by the treatment of cells with proteosomal inhibitor (Fig. 5B and C), suggesting that the degradation of all p130 species occurred in proteosome-dependent manner. We also observed that the levels of 1-6/A and 1-6/D mutant proteins were high in G_0/G_1-arrested cells, reduced upon the S-phase progression, and then up-regulated again as the cells entered G_1 phase, indicating their susceptibility to the cell cycle-dependent proteosomal degradation (Fig. 5A). GSK3 phosphorylation has been shown to decrease the stability of and target to proteosomal degradation several proteins implicated in cellular proliferation, including c-Myc (50), cyclin D1 (16), and β-catenin (49). Accumulation of these GSK3 substrates in the cells is linked to increased proliferation and is observed in different types of cancer. It is yet unclear whether the observed destabilization of a nonphosphorylated Loop mutant of p130 indicates an additional, proteosome-independent mechanism of regulation of p130 expression levels. We should point out that the effect of 1,3,5/A and 1-6/A mutations on the stability of p130 appears modest and could result from conformational changes. The fact that unlike the other GSK3 substrates mentioned above, destabilization of p130 was caused by lack of phosphorylation at the GSK3-targeted fragment indicates a novel way of GSK3-mediated regulation. Interestingly, a regulatory component of the adenomatous polyposis coli–β-catenin complex, axin, has been shown to be phosphorylated by GSK3, and this phosphorylation resulted in its stabilization while alanine substitution in the putative GSK3 sites resulted in destabilization of the mutant protein (58). To our knowledge, this is the only other example of stabilization of substrate protein caused by GSK3 phosphorylation besides our result from p130 described here. It would be intriguing to find out whether there is a common mechanism that regulates these two GSK3 targets.

Our data presented here identify p130 as a novel target of GSK3, adding to the list of the GSK3 substrates implicated into the control of cell proliferation. While we did not find a link between GSK3 phosphorylation of p130 and any known cell cycle regulatory functions of p130 or the cell cycle-dependent regulation of p130, our work sets the stage for further studies aimed at elucidating the physiological functions of these two intriguing proteins.

ACKNOWLEDGMENTS

We are grateful to William Hahn, Ralph Scully, and Hartmut Land for reagents.

This work was supported in part by Public Health Service grant RO1-CA63113 (J.D.).

REFERENCES

1. **Ausubel, F. M. (ed.).** 1999. Short protocols in molecular biology, 4th ed. John Wiley & Sons, Inc., New York, N.Y.
2. **Bhattacharya, S., J. Garriga, J. Calbo, T. Yong, D. S. Haines, and X. Grana.** 2003. SKP2 associates with p130 and accelerates p130 ubiquitylation and degradation in human cells. Oncogene **22:**2443–2451.
3. **Cam, H., and B. D. Dynlacht.** 2003. Emerging roles for E2F: beyond the G1/S transition and DNA replication. Cancer Cell **3:**311–316.
4. **Canhoto, A. J., A. Chestukhin, L. Litovchick, and J. A. DeCaprio.** 2000. Phosphorylation of the retinoblastoma-related protein p130 in growth-arrested cells. Oncogene **19:**5116–5122.
5. **Chestukhin, A., L. Litovchick, K. Rudich, and J. A. DeCaprio.** 2002. Nucleocytoplasmic shuttling of p130/RBL2: novel regulatory mechanism. Mol. Cell. Biol. **22:**453–468.
6. **Classon, M., and N. Dyson.** 2001. p107 and p130: versatile proteins with interesting pockets. Exp. Cell Res. **264:**135–147.
7. **Classon, M., S. Salama, C. Gorka, R. Mulloy, P. Braun, and E. Harlow.** 2000. Combinatorial roles for pRB, p107, and p130 in E2F-mediated cell cycle control. Proc. Natl. Acad. Sci. USA **97:**10820–10825.
8. **Cobrinik, D., M. H. Lee, G. Hannon, G. Mulligan, R. T. Bronson, N. Dyson, E. Harlow, D. Beach, R. A. Weinberg, and T. Jacks.** 1996. Shared role of the pRB-related p130 and p107 proteins in limb development. Genes Dev. **10:**1633–1644.
9. **Coghlan, M. P., A. A. Culbert, D. A. Cross, S. L. Corcoran, J. W. Yates, N. J. Pearce, O. L. Rausch, G. J. Murphy, P. S. Carter, L. Roxbee Cox, D. Mills, M. J. Brown, D. Haigh, R. W. Ward, D. G. Smith, K. J. Murray, A. D. Reith, and J. C. Holder.** 2000. Selective small molecule inhibitors of glycogen synthase kinase-3 modulate glycogen metabolism and gene transcription. Chem. Biol. **7:**793–803.
10. **Dajani, R., E. Fraser, S. M. Roe, N. Young, V. Good, T. C. Dale, and L. H. Pearl.** 2001. Crystal structure of glycogen synthase kinase 3 beta: structural basis for phosphate-primed substrate specificity and autoinhibition. Cell **105:**721–732.
11. **Dannenberg, J. H., A. van Rossum, L. Schuijff, and H. te Riele.** 2000. Ablation of the retinoblastoma gene family deregulates G(1) control causing immortalization and increased cell turnover under growth-restricting conditions. Genes Dev. **14**:3051–3064.
12. **Davies, S. P., H. Reddy, M. Caivano, and P. Cohen.** 2000. Specificity and mechanism of action of some commonly used protein kinase inhibitors. Biochem. J. **351:**95–105.
13. **Davis, R. J.** 1993. The mitogen-activated protein kinase signal transduction pathway. J. Biol. Chem. **268:**14553–14556.

14. **DeCaprio, J. A., J. W. Ludlow, J. Figge, J. Y. Shew, C. M. Huang, W. H. Lee, E. Marsilio, E. Paucha, and D. M. Livingston.** 1988. SV40 large tumor antigen forms a specific complex with the product of the retinoblastoma susceptibility gene. Cell **54:**275–283.
15. **Dick, F. A., E. Sailhamer, and N. J. Dyson.** 2000. Mutagenesis of the pRB pocket reveals that cell cycle arrest functions are separable from binding to viral oncoproteins. Mol. Cell. Biol. **20:**3715–3727.
16. **Diehl, J. A., M. Cheng, M. F. Roussel, and C. J. Sherr.** 1998. Glycogen synthase kinase-3beta regulates cyclin D1 proteolysis and subcellular localization. Genes Dev. **12:**3499–3511.
17. **Dyson, N.** 1998. The regulation of E2F by pRB-family proteins. Genes Dev. **12:**2245–2262.
18. **Dyson, N., K. Buchkovich, P. Whyte, and E. Harlow.** 1989. The cellular 107K protein that binds to adenovirus E1A also associates with the large T antigens of SV40 and JC virus. Cell **58:**249–255.
19. **Farkas, T., K. Hansen, K. Holm, J. Lukas, and J. Bartek.** 2002. Distinct phosphorylation events regulate p130- and p107-mediated repression of E2F4. J. Biol. Chem. **277:**26741–26752.
20. **Ferkey, D. M., and D. Kimelman.** 2000. GSK3: new thoughts on an old enzyme. Dev. Biol. **225:**471–479.
21. **Frame, S., P. Cohen, and R. M. Biondi.** 2001. A common phosphate binding site explains the unique substrate specificity of GSK3 and its inactivation by phosphorylation. Mol. Cell **7:**1321–1327.
22. **Garriga, J., A. Limon, X. Mayol, S. G. Rane, J. H. Albrecht, E. P. Reddy, V. Andres, and X. Grana.** 1998. Differential regulation of the retinoblastoma family of proteins during cell proliferation and differentiation. Biochem. J. **333:**645–654.
23. **Ghosh, M. K., and M. L. Harter.** 2003. A viral mechanism for remodeling chromatin structure in G0 cells. Mol. Cell **12:**255–260.
24. **Graña, X., J. Garriga, and X. Mayol.** 1998. Role of the retinoblastoma protein family, pRB, p107 and p130 in the negative control of cell growth. Oncogene **17:**3365–3383.
25. **Hahn, W. C., C. M. Counter, A. S. Lundberg, R. L. Beijersbergen, M. W. Brooks, and R. A. Weinberg.** 1999. Creation of human tumour cells with defined genetic elements. Nature **400:**464–468.
26. **Hansen, K., T. Farkas, J. Lukas, K. Holm, L. Ronnstrand, and J. Bartek.** 2001. Phosphorylation-dependent and -independent functions of p130 cooperate to evoke a sustained G1 block. EMBO J. **20:**422–432.
27. **Hansen, K., J. Lukas, K. Holm, A. A. Kjerulff, and J. Bartek.** 1999. Dissecting functions of the retinoblastoma tumor suppressor and the related pocket proteins by integrating genetic, cell biology, and electrophoretic techniques. Electrophoresis **20:**372–381.
28. **Harwood, A. J.** 2001. Regulation of GSK3: a cellular multiprocessor. Cell **105:**821–824.
29. **Herrera, R. E., V. P. Sah, B. O. Williams, T. P. Mäkelä, R. A. Weinberg, and T. Jacks.** 1996. Altered cell cycle kinetics, gene expression, and G_1 restriction point regulation in *Rb*-deficient fibroblasts. Mol. Cell. Biol. **16:**2402–2407.
30. **Lacy, S., and P. Whyte.** 1997. Identification of a p130 domain mediating interactions with cyclin A/cdk 2 and cyclin E/cdk 2 complexes. Oncogene **14:**2395–2406.
31. **LeCouter, J. E., B. Kablar, W. R. Hardy, C. Ying, L. A. Megeney, L. L. May, and M. A. Rudnicki.** 1998. Strain-dependent myeloid hyperplasia, growth deficiency, and accelerated cell cycle in mice lacking the Rb-related *p107* gene. Mol. Cell. Biol. **18:**7455–7465.
32. **LeCouter, J. E., B. Kablar, P. F. Whyte, C. Ying, and M. A. Rudnicki.** 1998. Strain-dependent embryonic lethality in mice lacking the retinoblastoma-related p130 gene. Development **125:**4669–4679.
33. **Lee, D. H., and A. L. Goldberg.** 1996. Selective inhibitors of the proteasome-dependent and vacuolar pathways of protein degradation in Saccharomyces cerevisiae. J. Biol. Chem. **271:**27280–27284.
34. **Lee, M. H., B. O. Williams, G. Mulligan, S. Mukai, R. T. Bronson, N. Dyson, E. Harlow, and T. Jacks.** 1996. Targeted disruption of p107: functional overlap between p107 and Rb. Genes Dev. **10:**1621–1632.
35. **Li, Y., C. Graham, S. Lacy, A. M. Duncan, and P. Whyte.** 1993. The adenovirus E1A-associated 130-kD protein is encoded by a member of the retinoblastoma gene family and physically interacts with cyclins A and E. Genes Dev. **7:**2366–2377.
36. **Lipinski, M. M., and T. Jacks.** 1999. The retinoblastoma gene family in differentiation and development. Oncogene **18:**7873–7882.
37. **Mayol, X., J. Garriga, and X. Graña.** 1995. Cell cycle-dependent phosphorylation of the retinoblastoma-related protein p130. Oncogene **11:**801–808.
38. **Mayol, X., J. Garriga, and X. Graña.** 1996. G1 cyclin/CDK-independent phosphorylation and accumulation of p130 during the transition from G1 to G0 lead to its association with E2F4. Oncogene **13:**237–246.
39. **Morgenstern, J. P., and H. Land.** 1990. Advanced mammalian gene transfer: high titre retroviral vectors with multiple drug selection markers and a complementary helper-free packaging cell line. Nucleic Acids Res. **18:**3587–3596.
40. **Mulligan, G., and T. Jacks.** 1998. The retinoblastoma gene family: cousins with overlapping interests. Trends Genet. **14:**223–229.
41. **Naerum, L., L. Norskov-Lauritsen, and P. H. Olesen.** 2002. Scaffold hopping and optimization towards libraries of glycogen synthase kinase-3 inhibitors. Bioorg. Med. Chem. Lett. **12:**1525–1528.
42. **Pear, W. S., G. P. Nolan, M. L. Scott, and D. Baltimore.** 1993. Production of high-titer helper-free retroviruses by transient transfection. Proc. Natl. Acad. Sci. USA **90:**8392–8396.
43. **Plyte, S. E., K. Hughes, E. Nikolakaki, B. J. Pulverer, and J. R. Woodgett.** 1992. Glycogen synthase kinase-3: functions in oncogenesis and development. Biochim. Biophys. Acta **1114:**147–162.
44. **Reynolds, C. H., J. C. Betts, W. P. Blackstock, A. R. Nebreda, and B. H. Anderton.** 2000. Phosphorylation sites on tau identified by nanoelectrospray mass spectrometry: differences in vitro between the mitogen-activated protein kinases ERK2, c-Jun N-terminal kinase and P38, and glycogen synthase kinase-3beta. J. Neurochem. **74:**1587–1595.
45. **Rossi, F., H. E. MacLean, W. Yuan, R. O. Francis, E. Semenova, C. S. Lin, H. M. Kronenberg, and D. Cobrinik.** 2002. p107 and p130 coordinately regulate proliferation, Cbfa1 expression, and hypertrophic differentiation during endochondral bone development. Dev. Biol. **247:**271–285.
46. **Ruiz, S., C. Segrelles, A. Bravo, M. Santos, P. Perez, H. Leis, J. L. Jorcano, and J. M. Paramio.** 2003. Abnormal epidermal differentiation and impaired epithelial-mesenchymal tissue interactions in mice lacking the retinoblastoma relatives p107 and p130. Development **130:**2341–2353.
47. **Ryves, W. J., and A. J. Harwood.** 2001. Lithium inhibits glycogen synthase kinase-3 by competition for magnesium. Biochem. Biophys. Res. Commun. **280:**720–725.
48. **Sage, J., G. J. Mulligan, L. D. Attardi, A. Miller, S. Chen, B. Williams, E. Theodorou, and T. Jacks.** 2000. Targeted disruption of the three Rb-related genes leads to loss of G(1) control and immortalization. Genes Dev. **14:**3037–3050.
49. **Salic, A., E. Lee, L. Mayer, and M. W. Kirschner.** 2000. Control of beta-catenin stability: reconstitution of the cytoplasmic steps of the wnt pathway in Xenopus egg extracts. Mol. Cell **5:**523–532.
50. **Sears, R., F. Nuckolls, E. Haura, Y. Taya, K. Tamai, and J. R. Nevins.** 2000. Multiple Ras-dependent phosphorylation pathways regulate Myc protein stability. Genes Dev. **14:**2501–2514.
51. **Smith, E. J., G. Leone, J. DeGregori, L. Jakoi, and J. R. Nevins.** 1996. The accumulation of an E2F-p130 transcriptional repressor distinguishes a G_0 cell state from a G_1 cell state. Mol. Cell. Biol. **16:**6965–6976.
52. **Smith, E. J., G. Leone, and J. R. Nevins.** 1998. Distinct mechanisms control the accumulation of the Rb-related p107 and p130 proteins during cell growth. Cell Growth Differ. **9:**297–303.
53. **Stevaux, O., and N. J. Dyson.** 2002. A revised picture of the E2F transcriptional network and RB function. Curr. Opin. Cell Biol. **14:**684–691.
54. **Tedesco, D., J. Lukas, and S. I. Reed.** 2002. The pRb-related protein p130 is regulated by phosphorylation-dependent proteolysis via the protein-ubiquitin ligase SCF(Skp2). Genes Dev. **16:**2946–2957.
55. **ter Haar, E., J. T. Coll, D. A. Austen, H. M. Hsiao, L. Swenson, and J. Jain.** 2001. Structure of GSK3beta reveals a primed phosphorylation mechanism. Nat. Struct. Biol. **8:**593–596.
56. **Whyte, P., K. J. Buchkovich, J. M. Horowitz, S. H. Friend, M. Raybuck, R. A. Weinberg, and E. Harlow.** 1988. Association between an oncogene and an anti-oncogene: the adenovirus E1A proteins bind to the retinoblastoma gene product. Nature **334:**124–129.
57. **Woodgett, J. R.** 2001. Judging a protein by more than its name: GSK3. Sci. STKE **2001:**RE12. [Online.] http://stke.sciencemag.org.
58. **Yamamoto, H., S. Kishida, M. Kishida, S. Ikeda, S. Takada, and A. Kikuchi.** 1999. Phosphorylation of axin, a Wnt signal negative regulator, by glycogen synthase kinase-3beta regulates its stability. J. Biol. Chem. **274:**10681–10684.
59. **Zalvide, J., and J. A. DeCaprio.** 1995. Role of pRb-related proteins in simian virus 40 large-T-antigen-mediated transformation. Mol. Cell. Biol. **15:**5800–5810.
60. **Zhang, S., X. Qian, C. Redman, V. Bliskovski, E. S. Ramsay, D. R. Lowy, and B. A. Mock.** 2003. p16 INK4a gene promoter variation and differential binding of a repressor, the ras-responsive zinc-finger transcription factor, RREB. Oncogene **22:**2285–2295.
61. **Zhang, S., E. S. Ramsay, and B. A. Mock.** 1998. Cdkn2a, the cyclin-dependent kinase inhibitor encoding p16INK4a and p19ARF, is a candidate for the plasmacytoma susceptibility locus, Pctr1. Proc. Natl. Acad. Sci. USA **95:**2429–2434.